4

High Efficiency Red Phosphorescent Organic Light-Emitting Diodes with Simple Structure

Ramchandra Pode[1] and Jang Hyuk Kwon[2]
[1]*Department of Physics*
[2]*Department of Information Display*
Kyung Hee University
Korea

1. Introduction

After the first report of electroluminescence in anthracene organic materials in monolayer devices in 1963 by Pope et al. (Pope et al., 1963) and by Helfrich and Schneider in 1965 (Helfrich & Schneider, 1965), this phenomenon remained of pure academic interest for the next two decades owing to the difficulty of growing large-size single crystals and the requirement of a very high voltage (~ 1000 V) to produce the luminance. The evolution of OLED devices is summarized in Fig. 1. Tang and his group demonstrated that the poor performance of the monolayer early device was dramatically improved in two layers device by the addition of a hole transport layer (HTL) with the thin amorphous film stacking in the device structure (VanSlyke & Tang, 1985; Tang et al., 1988). Organic electroluminescent devices having improved power conversion efficiencies by doping the emitting layer were also realized around the same time by the Kodak group. Subsequently, heterostructure configurations to improve the device performance were implemented by inserting several layers like buffer layer between anode and hole transport layer (HTL) (VanSlyke et al., 1996; Shirota et al., 1994; Deng et al., 1999) electron transport layer (ETL), hole blocking layer (HBL) (Adamovich et al., 2003) or interlayer between cathode and ETL (Hung et al., 1997; Kido and Lizumi, 1998) in the device structure. Such multilayer device structure often enhances the drive voltages of OLEDs. Usually, the operating voltage for higher brightness was much higher than the thermodynamic limit which is 2.4 eV for a green device. Chemical doping with either electron donors (for electron transport materials) or electron acceptors (for hole transport materials) can significantly reduce the voltage drop across these films. These devices with either HTL or ETL doped layer show improved performance; but the operating voltages were still rather higher than the thermodynamic limit. Subsequently, Leo and his group proposed the concept of p-type doped HTL and n-type doped ETL (J. Huang et al., 2002). These p-i-n structure devices show high luminance and efficiency at extremely low operating voltages. Indeed all these devices have multilayer structure with high current- and power-efficiencies, but thin emitting layer. Nevertheless, narrow thickness of emitting layer in p-i-n OLEDs and complex design architecture of phosphorescent OLEDs are not desirable from the manufacturing perspective.

In recent years, white phosphorescent OLEDs (PHOLEDs) have received a great deal of attention owing to their potential use in high performance and brightness displays, solid state lighting, and back lighting for Liquid Crystal Displays. White emission can be achieved by mixing three primary colors (red, green, and blue) (D'Andrade et al., 2004; Holmes et al. 2003) or two complementary colors from different emitters (Li et al., 2003; J. Liu et al., 2006; Al Attar et al., 2005). Issues of undesired chromaticity as well as poor batch-to-batch reproducibility resulting in low image quality displays in three colors mixing white OLEDs, are minimized in two colors mixing involving an orange emitter complemented with a blue emitter to produce a white light using a combination of fluorescent/phosphorescent or phosphorescent/phosphorescent emitters in doped OLEDs. Consequently, the demand for the efficient true red bright color for multiple color display and lighting purposes has been significantly enhanced. Indeed, interest in employing red emitters in combination with blue emitters to achieve a white light emission with the simpler OLED architecture is spurred in recent days (Li et al., 2003; J. Liu et al., 2006; Al Attar et al., 2005; Seo et al., 2007; Ho et al., 2008a, 2008b; Chen et al., 2008; Shoustikov et al., 1997).

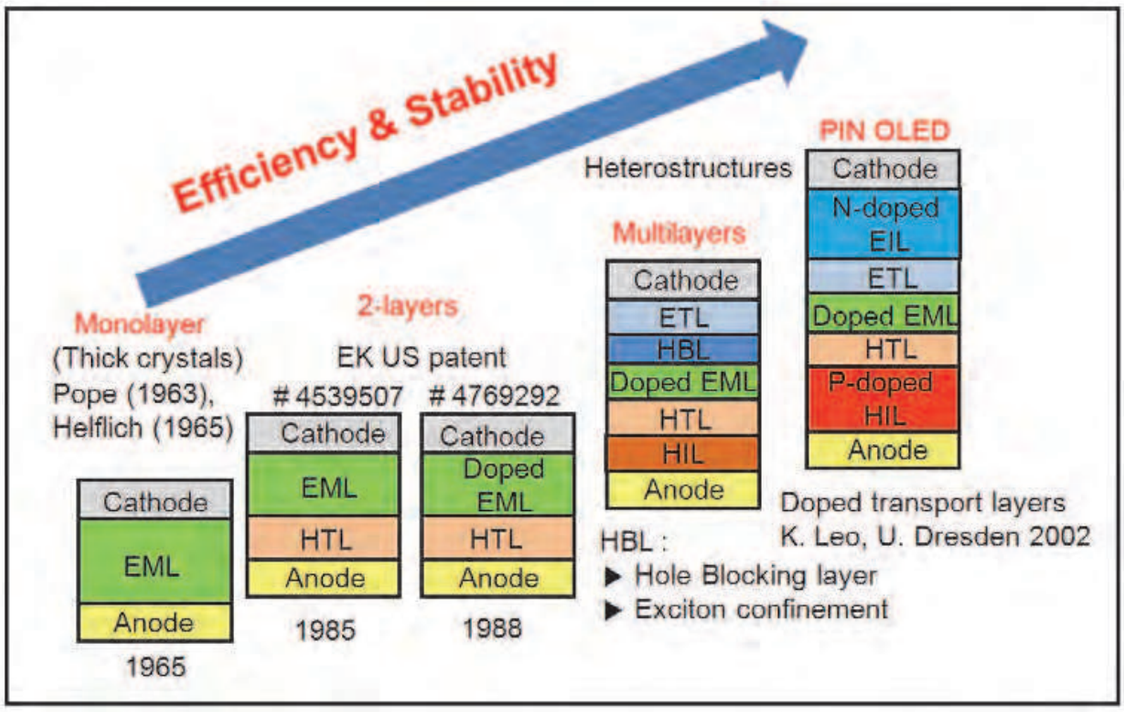

Fig. 1. Evolution of OLED devices (HIL: hole injection layer, HTL: hole transport layer, EML: emissive layer, HBL: hole blocking layer, ETL: electron transport layer)

In this chapter, we discuss efficient red phosphorescent organic light-emitting diodes implemented using multiple quantum well structure, two layers, single layer structures, and ideal host and guest system configurations. The importance of the topic is discussed in this section. The current status of phosphorescent red OLEDs, multiple quantum well, two layers, and single layer configurations for red PHOLEDs are discussed in sections 2, 3, 4, and 5, respectively. Ideal host and guest system for the optimum performance of the red PHOLEDs is presented in section 6. Finally, the conclusion of the present study is illustrated in the section 7 of this chapter.

2. Phosphorescent OLED devices

In recent years, phosphorescent organic light-emitting devices (PHOLEDs) are acquiring the mainstream position in the field of organic displays owing to their potential use in high brightness applications. Schematic of phosphorescence OLEDs and emission mechanism are displaced in Fig. 2. An upper limit on the external quantum efficiency of 5 % in fluorescent small molecule organic devices has been overcome in PHOLEDs by harvesting the singlet and triplet excitons to emission of photons (Baldo et al., 1998; Adachi et al., 2001a). A PHOLED with an internal quantum efficiency of nearly 100% has been demonstrated due to the harvest of both singlet and triplet excitons, leading to devices with high efficiencies (Adachi et al., 2001b; Ikai et al., 2001; Fukase and Kido, 2002; Williams et al., 2007). To achieve the high quantum efficiency in phosphorescent OLEDs, the excited energy of the phosphorescent emitter has to be confined within the emitter itself using wide-energy-gap host materials and carrier-transporting materials, which have higher triplet excited energy levels than that of the emitter and multilayer architecture comprising electron/hole injection and transport layers as shown in Fig. 2. Such multilayer structure often enhances the drive voltages of PHOLEDs. The turn-on voltage of conventional PHOLEDs is relatively high about 1 ~ 2 V compared to that of fluorescent OLEDs as the device designed has multilayer structures for good charge balance and excitons confinement within an emitting material layer (EML), limiting their use in display industries (Wakimoto et al., 1997; Endo et al., 2002).

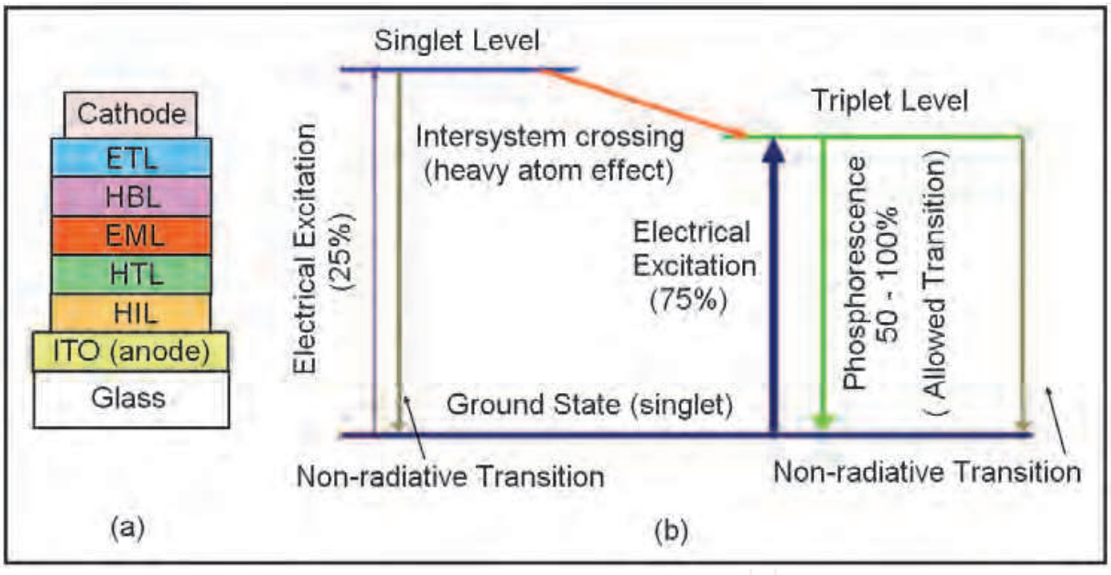

Fig. 2. (a) Schematic of small molecule based phosphorescence OLED, (b) Phosphorescence emission mechanism in phosphorescent OLEDs.

Usually, wide energy gap 4,4′-bis(N-carbazolyl)-1,1′-biphenyl (CBP) is used as a host material for red (~ 2.0 eV) or green (~ 2.3 – 2.4 eV) phosphorescent guests. Iridium (III) and platinum (II) phosphorescent emitters are widely used as triplet dopants molecule. Various red emitting Ir(III) phosphorescent complexes are summarized in Table 1 (Lamansky et al., 2001; Tsuboyama et al., 2003; Duan et al., 2003; H.-K. Kim et al., 2007; Ohmori et al., 2007; J. Huang et al., 2007; Tsuzuki and Tokito, 2008; Mi et al., 2009; T.-C. Lee et al., 2009; Pode et al., 2010; K.-K. Kim et al., 2010; Tsujimoto et al., 2010). The wide band gap host and narrow band gap (E_g)

guest red light emitting system has a significant difference in HOMO (highest occupied molecular orbital) and/or LUMO (lowest unoccupied molecular orbital) levels between the guest and host materials. Thus, the guest molecules are thought to act as *deep traps for electrons and holes in the emitting layer*, causing an increase in the drive voltage of the PHOLED. Further, the dopant concentration in such a host-guest system is usually as high as about 6 ~ 10 percent by weight (wt%) because injected charges move through dopant molecules in the emitting layer. Therefore, self-quenching or triplet-triplet annihilation by dopant molecules is an inevitable problem in host-guest systems with high doping concentrations. Table 2 shows the material performance of red emitting small molecule and polymer PHOLEDs. Table 3 illustrates the suppliers of various materials used in PHOLEDs fabrication.

Sr. No.	Ir complex	Soluble in	Emission wavelength (nm)	Ref.
1)	$Ir(btp)_2(acac)$	2-methyltetrahydrofur-an	612 (PL)	Lamansky et al., 2001
2)	$Ir(piq)_3$	toluene	620	Tsuboyama et al., 2003
3)	$Ir(DBQ)_2(acac)$ $Ir(MDQ)_2(acac)$	CH_2Cl_2	618 (PL) 608 (PL)	Duan et al., 2003
4)	$Ir(piq)_3$	1,2-dichlorobenzene	620	H.-K. Kim et al., 2007
5)	$Ir(piq)_3$	1,2-dichlorobenzene	630	Ohmori et al., 2007
6)	$Ir(C8piq)_3$ $Ir(4F5mpiq)_3$ [F = Fluorine, M = methyl	p-xylene	621 608	J. Huang et al., 2007
7)	$Ir(C4\text{-}piq)_3$	1,2-dichlorobenzene	619 or 617	Tsuzuki and Tokito, 2008
8)	$Ir(BPPa)_3$	CH_2Cl_2	625 (PL)	Mi et al., 2009
9)	$(piq)_2Ir(PO)$ $(nazo)_2Ir(PO)$ $(piq)Ir(PO)_2$ $(nazo)Ir(PO)_2$	CH_2Cl_2	652 (PL) 657 (PL) 591, 620 (PL) 690 (PL)	T.-C. Lee et al., 2009
10	i) $(Et\text{-}Cvz\text{-}PhQ)_2Ir(pic)$ ii)$(EO\text{-}Cvz\text{-}PhQ)_2Ir(picN\text{-}O)$ iii) $(EO\text{-}Cvz\text{-}PhQ)_2Ir(pic)$	1,2-dichlorobenzene	600	Pode et al., 2010
11	$(Ir(phq)_2acac)$ $Ir(piq)_2acac$	1,2-dichlorobenzene	596 and 597	K.-K. Kim et al., 2010
12	$Ir(dbfiq)_2(bdbp)$	Toluene Device	640 (PL) 636 to 642	Tsujimoto et al., 2010

PL : Photoluminescence

Table 1. Red emitting phosphorescent Ir complexes

Device	Lifetime (t50) (h)	Efficacy (cd/A)	Source
Small molecule (Ph) @1000 cd/m²	120 – 500K	22 – 28	Universal Display
Polymer @1000 cd/m²	200 – 350K	11 – 31	CDT

Table 2. Red materials performance, 2009

Light Emitting Hosts and Dopants	Injectors/Transporters
• Cambridge Display Technology – Polymers • DuPont – Solution Based Phosphorescent small Molecule • Idemitsu Kosan – Fluorescent and Phosphorescent Small Molecule • Merck – Polymers, Small Molecule • Universal Display – Phosphorescent Small Molecule • Dow Chemical – Fluorescent and Phosphorescent Small Molecule • Sunfine Chem – Fluorescent and Phosphorescent Small Molecule • LG Chemical – Fluorescent Small Molecule	• DS Himetal Dow Chemical • H.C. Starck Group • LG Chemical • Cheil Industries Inc. • Toray • Merck • Nippon Steel Chemical Co., Ltd. • Nissan Chemical Industries • Novaled – P/N Doping • Plextronics • BASF

Table 3. Organic Materials Suppliers

Although PHOLEDs are becoming increasingly important for high brightness displays and lighting applications, there are several issues which need to be addressed sooner or later such as:

- Complex architecture (Multilayer Structure)
- High driving voltage
- Low power efficiency
- Interfacial barrier and charge built-up at interfaces
- Poor performance at driving current densities exceeding 1 mA/cm²
- Doping concentration about 6 ~ 10 wt%
- Cost competitiveness.

Earlier, Kawamura et al. had reported that the phosphorescence photoluminescence quantum efficiency of $Ir(ppy)_3$ could be decreased by ~5% with an increasing in doping concentration from 2 to 6% (Kawamura et al., 2006). Consequently, the selection of suitable host candidates is a critical issue in fabricating high efficiency PHOLEDs. More recently in order to address device performance and manufacturing constraints, an ideal host-guest system to produce a high efficiency phosphorescent device using a narrow band gap fluorescent host to prevent the hole/or electron trapping has been presented (Jeon et al., 2008a, 2008b; Jeon et al., 2009; Pode et al., 2009). A class of narrow band gap fluorescent material utilizing beryllium complexes as host and ETL for efficient red phosphorescent

devices has been proposed. Characteristics of narrow band-gap phosphorescent hosts are: (1) *Small energy band gap,* (2) *Small energy gap between singlet state and triplet state, and* (3) *Good electron transport characteristic.* Simple structure red PHOLED, using narrow band gap fluorescent host materials has demonstrated a *high device performance* and *low manufacturing cost.*

3. Multiple quantum well structure

3.1 Introduction

Organic light emitting diodes (OLEDs) have attracted considerable attention because of their potential applicability to flat-panel displays (FPDs) (Sheats et al., 1996; Shen et al., 1997; Friend et al., 1999), backlighting, and candidates for the next generation lighting (Destruel et al., 1999; D'Andrade and Forrest, 2004), owing to wide viewing angle, low driving voltage, thin, light-weight, and possibly also flexible displays. Indispensable requirement for these applications is the high efficiency of OLEDs devices. In order to achieve the high efficiency in OLEDs, various approaches such as use of highly efficient (high luminescence quantum efficiency) organic materials, insertion of the excition blocking layer and/or hole and electron blocking layers, and optimization of the doping concentration of OLEDs to reduce self-quenching have been reported (Baldo et al., 1998; Bulovic et al., 1998; Baldo et al., 1999). Among these approaches, especially exciton confinement approach by introducing a carrier and/or exciton blocking layer(s) is the most effective and mainly used until now.

Quantum confinement approach using a multiple quantum well (MQW) structure or multi-quantum barrier is widely used in inorganic LED as it leads to a higher efficiency compared to the double hetero- structure or single quantum well (QW) structure. While in OLEDs, only few reports about the MQW structure with good carrier confinement ability were presented till to date. Qiu et al. (Qiu et al., 2002a; 2002b) and Huang et al. (J. Huang et al., 2000) have reported the organic MQW structure by using copper phthalocyanine (CuPc) and N,N'-bis(1-naphthyl)-N,N'-diphenyl-1,1'-biphenyl-4,4'-diamine (NPB) or rubrene. In these articles, the MQW effect has been reported in the fluorescent devices, wherein real device efficiency is not so high besides the poor emission color stability. Recently, the triplet quantum well structure has been reported by Kim et al. using a 4,4'-bis(N-carbazolyl)-1,10-biphenyl (CBP) and PH1 host (S. H. Kim et al., 2007). Since $Ir(ppy)_3$ was doped in all quantum well layers, charge carriers couldn't be effectively confined in this device as carriers move via dopant molecules. Consequently, stable high efficiency results in such a MQW structure couldn't be realized.

In this section, we report the real MQW device structure having various triplet quantum well devices from a single to five quantum wells. Owing to confinement of the triplet energy at the emitting layers in the fabricated MQW device, the highest phosphorescent efficiency is obtained among reported tris(1-phenylisoquinoline)iridium ($Ir(piq)_3$) dopant OLEDs (H. Kim et al., 2008) with a very good color emission stability. The MQW structure is realized using a wide band-gap hole and electron transporting layers, narrow band-gap host and dopant materials, and charge control layers (CCL). Bis(10-hydroxybenzo[h] quinolinato)beryllium complex ($Bebq_2$) and bis[2-(2-hydroxyphenyl)-pyridine] beryllium ($Bepp_2$) are used as a narrow band-gap host material and a CCL material, respectively.

3.2 Experimental

Figure 3(a) shows the configuration of fabricated red PHOLEDs, having a MQW structure. Here, n consists of [$Bebq_2$:$Ir(piq)_3$/ CCL] (red electroluminescence (R-EL) unit) varying from

1 to 5. The 40 nm thick 4, 4′, 4″-tri(N-carbazolyl)triphenylamine (TCTA) hole transport layer (HTL) doped with WO_3 (doping concentration 30 %) is deposited on an indium tin oxide (ITO) coated glass substrate. To prevent the non-radiative quenching of triplet excitons generated at the heavily doped HTL, an electron blocking buffer layer of 12 nm thick TCTA was deposited. Subsequently, emissive layers (EMLs) with quantum-well structures were deposited. The emission layer structures of PHOLEDs were increased by adding the R-EL unit. In order to confine and control a hole and electron in the EML, the CCL layer with a thickness of 5 nm was deposited inside of EML. Later, $Bepp_2$ hole and exciton blocking buffer layer was deposited and followed by a 10 % Cs_2CO_3-doped $Bepp_2$ electron transport layer (ETL). The triplet energies of TCTA, $Bepp_2$, $Bebq_2$, and $Ir(piq)_3$ are 2.7, 2.7, 2.2, and 2.0 eV, respectively (Jeon et al., 2009; S. Y. Kim et al., 2009; Tsuboi et al., 2009). As triplet energies of charge carrier layers and CCL are higher than the host molecule (Fig. 3(b)), all triplet energies are confined in the emitting layers. Finally, Al cathode was deposited in another deposition chamber without breaking the vacuum. Deposition rate of Al was 5~10 Å/sec. The devices were fabricated on ITO coated glass with a sheet resistance of 20 Ω/ϒ. The substrates were cleaned with acetone and isopropyl alcohol sequentially, rinsed in de-ionized water, and then treated in UV-ozone immediately before loading into the high vacuum chamber (~ 2×10^{-7} Torr). The current density-voltage (J–V) and luminance–voltage (L–V) data of red PHOLEDs were measured by Keithley 2635 A and Minolta CS-1000A, respectively. The red PHOLED emitting area was 2 mm^2 for all the samples studied in the present work.

3.3 Results & discussion

In order to select the best CCL, we fabricated red PHOLEDs (n=2) with different CCL materials (CBP; device B, TCTA; device C, $Bepp_2$; device D) at the fixed CCL thickness of 5 nm. Device A was made without any CCL. In J-V-L results (not reproduced here), all three devices were measured until 10,000 cd/m^2 brightness value. The driving voltages (at 1000 cd/m^2) of these devices A, B, C and D are 3.8, 5.6, 6.0 and 4.2 V, respectively. As expected, the driving voltage increases by inserting the CCL. The external quantum efficiency (EQE) characteristics are shown in Fig. 4(a). At a given constant luminance of 1000 cd/m^2, the EQE values are 10.8, 5.1, 5.2, and 13.8 % for the devices A, B, C, and D, respectively. The EQE of the device D with $Bepp_2$ CCL is significantly higher than those of devices A~C. The HOMO energy levels of $Ir(piq)_3$, $Bebq_2$, CBP, TCTA and $Bepp_2$ were at 5.1 eV, 5.5 eV, 5.9 eV, 5.8 eV, and 5.7 eV, respectively. While the LUMO energy levels of $Ir(piq)_3$, $Bebq_2$, CBP, TCTA and $Bepp_2$ were at 3.1 eV, 2.8 eV, 2.6 eV, 2.4 eV, and 2.6 eV respectively. With the TCTA and CBP CCL layers devices, the deep HOMO and high LUMO levels of TCTA and CBP block the movement of holes and electrons at the $Bebq_2$:$Ir(piq)_3$/CCL interface. Therefore, holes and electrons cannot be easily transported through the CCL, resulting in the rise of driving voltage and efficiency decrease. However, the suitable HOMO and LUMO energy levels in $Bepp_2$ CCL can control the carrier movement at ease. As a result, $Bepp_2$ CCL partially confines holes and electrons at the first EML and some of holes and electrons arrive at the second EML after transporting through the $Bepp_2$ CCL. The CCL thickness is varied to optimize device characteristics from 3~10nm. The 5nm thickness of $Bepp_2$ CCL shows reasonable efficiency and voltage increase values.

In our double QW devices, hole barriers by CCLs are probably a dominant factor to control the current flow as hole barriers between HOMO levels of dopant and CCL are relatively high compared with electron barriers. Usually electrons easily overcome its barriers.

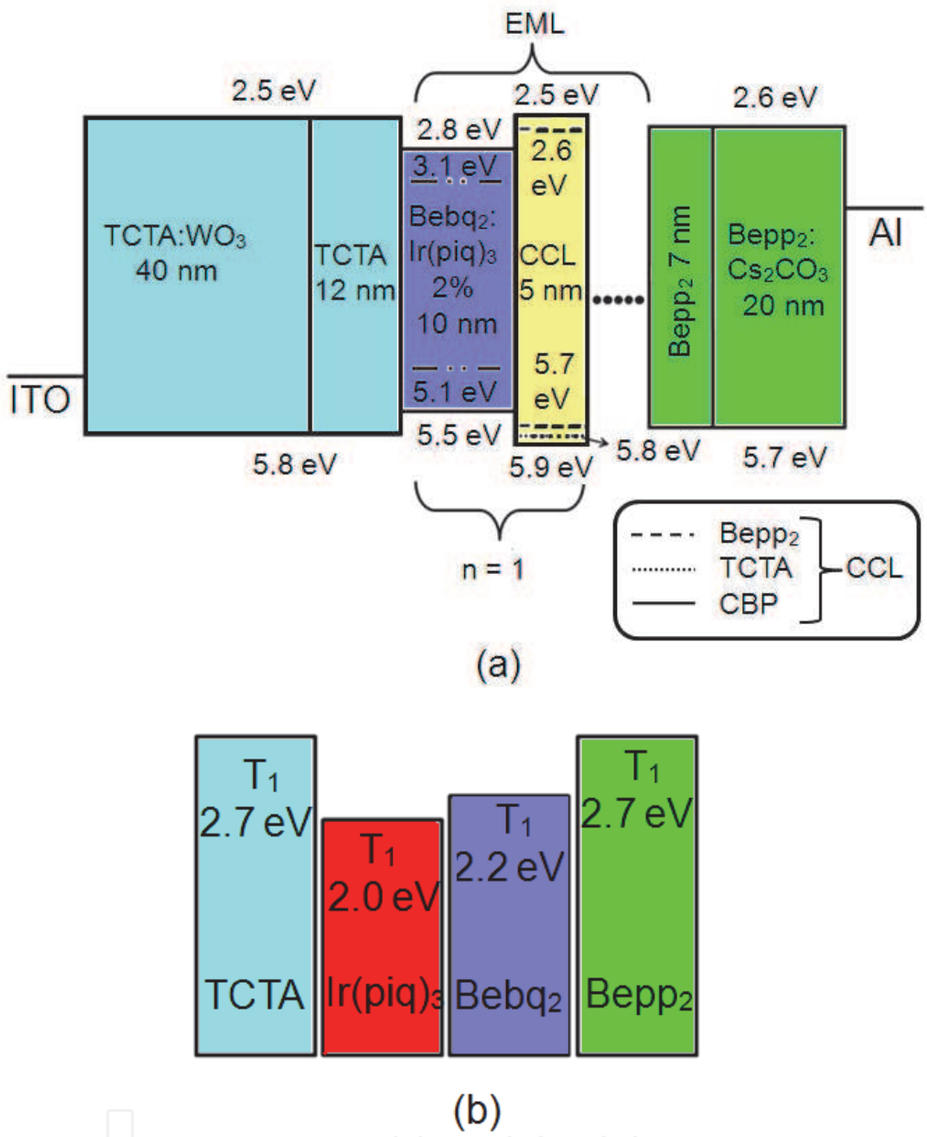

Fig. 3. (a) Energy band diagrams of fabricated red PHOLEDs with multiple quantum well structures. (b)Triplet energies of materials used in the present study.

In order to estimate the carrier confinement percentage in each EMLs with different CCL in double QW structure, the current density values are compared with the hole barriers obtained between HOMO levels of each CCL and $Ir(piq)_3$. According to the thermionic emission barrier model (Hong et al., 2005), ln(J) has a good linear relationship with the potential barrier (Φ).

Figure 4(b) shows a good agreement between Δln(J) and ΔΦ at 5V, indicating that the hole barrier is the main factor to determine the current flow in our devices. Here Δln(J) was calculated from the current density differences of single QW and double QW devices at 5 V and ΔΦ is the HOMO energy levels difference between the dopant and CCL. Almost similar behaviors are noticed at various voltages. Due to lower hole barrier with $Bepp_2$ compared with other CCL materials, the current flow is much easier with no hindrance. Hole carriers

can over-flow in the $Bepp_2$ CCL, creating more excitons in the double QW structure. Therefore, the device D with the $Bepp_2$ CCL improves the recombination efficiency of the electron-hole pairs.

Indeed, the efficiency with two quantum well device structure with $Bepp_2$ CCL is significantly improved. Further to investigate the influence of the quantum wells on the device performance, if any, we have fabricated PHOLEDs with MQW from 1 to 5 wells.

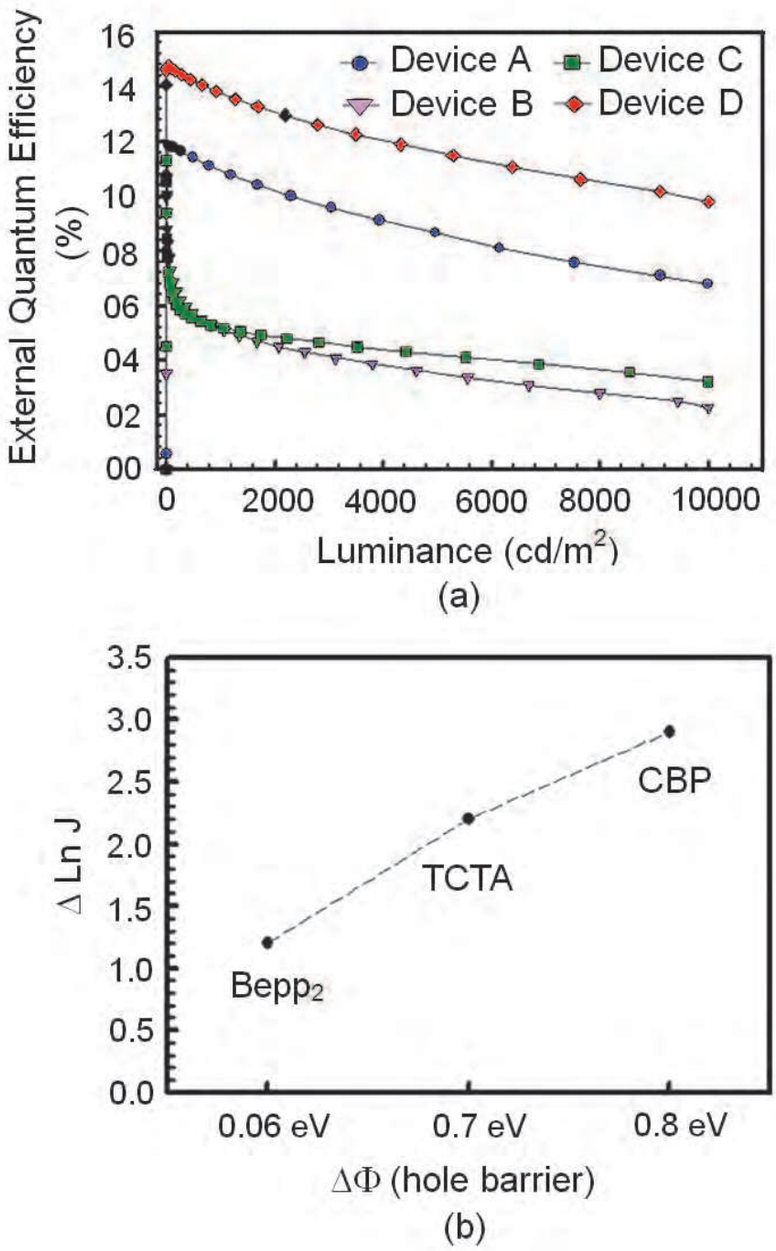

Fig. 4. (a) EQE characteristics of fabricated red PHOLEDs with and without CCL. (b) The current density difference between single quantum well device and double quantum well devices with different CCL

Figure 5 shows the J-V-L characteristics of fabricated red PHOLEDs with the increasing number of R-EL units from 1 to 5. The turn on voltages of MQW red PHOLEDs are 2.4 V for n=1 (device A), 2.5 V for n=2 (device D), 2.6 V for n=3, 2.8 V for n=4, and 3.2 V for n=5, respectively. The driving voltage to reach 1000 cd/m² is 3.8 V for n=1, 4.2 V for n=2, 4.8 V for n=3, 6.0 V for the n=4, and 7.4 V for n=5. The operating voltages in the MQW structure were increased by increasing the number of R-EL units because any addition of QW units offers additional resistance to the conduction of current. From Δln (J) data between single QW and double QW, we have calculated that 29% hole carriers can go the second EML through a $Bepp_2$ CCL.

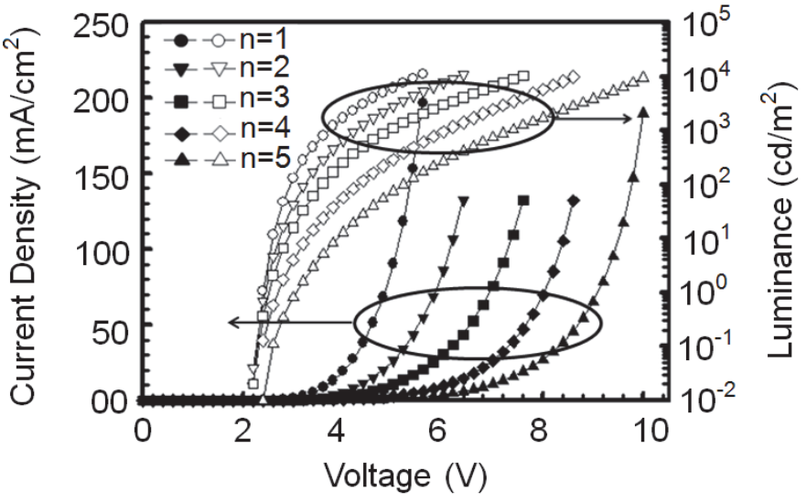

Fig. 5. J-V-L characteristics of fabricated red PHOLEDs with increasing R-EL unit from 1 to 5.

Figure 6 shows the maximum EQE characteristics of fabricated five red PHOLEDs while various electrical parameters of these devices are summarized in Table 4. The maximum EQE characteristics are 11.8 % for n=1, 14.8 % for n=2, 13.6 % for n=3, 12.8 % for n=4, and 8.6 % for n=5, respectively. *The best EL performances are obtained with n=2 among the five red PHOLEDs.* The over-flowing ratio of hole carriers with repeating additional QW and $Bepp_2$ CCL are shown in the inset of Fig. 6. From the J-V characteristics as displayed in Fig. 5, the over-flowing ratio of hole is estimated as [J(n=2)/J(n=1)] x 100% at 5 V (i.e. (90.40 mA/cm² / 26.39 mA/cm²) x 100% = 29%). Only 29% of hole carriers can reach to the second EML through a $Bepp_2$ CCL. The simple calculation results for n=3 and 4 were obtained by assuming 29% hole carrier overflow result for n=2. Real experimental data obtained from the J-V characteristics at 5V well agree with the calculated results, indicating our carrier overflow assumption is reasonable. The excitons can be confined upto 71% in the first QW existing adjacent to the TCTA buffer layer and 21% excitons in to the next second QW. The most excitons can be confined in first and second QWs. Therefore, the best EL performances seem to be obtained with n=2. By increasing the number of quantum wells to n=3 and n=4, the efficiency drop is not significant (over 12%) because electrons can reach to first and second QWs due to the negligible barrier to electron transport. However, the driving voltage is enhanced with increasing the number of QW structures and eventually 5 QW structure does not work properly. In our MQW devices, all devices show excellent color stability with the same CIE coordinate as (0.66, 0.33) as shown Table 4. Our results reveal

that the MQW structure improves the external quantum efficiency with no change in the CIE coordinate of red emitting PHOLEDs.

3.4 Conclusions

In summary, the maximum external quantum efficiency of 14.8 % with a two quantum well device structure is obtained, which is the highest value among the reported $Ir(piq)_3$ dopant red phosphorescent OLEDs.

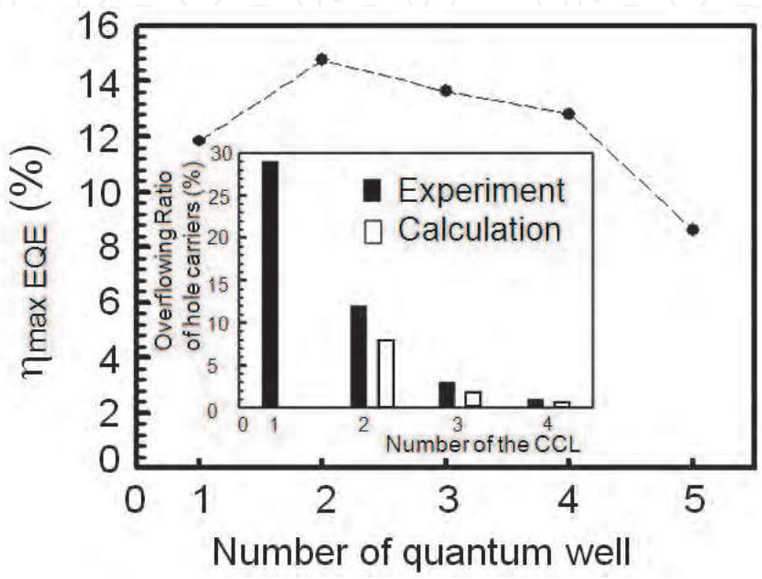

Fig. 6. Maximum EQE characteristics of fabricated five red PHOLEDs with increasing R-EL unit from 1 to 5. Inset: Overflowing ratios of hole carriers with increasing R-EL units.

Parameters	n=1	n=2	n=3	n=4	n=5
Turn on voltage (@ 1cd/m²)	2.4 V	2.5 V	2.6 V	2.8 V	3.2 V
Operating voltage (@ 1000 cd/m²)	3.8 V	4.2 V	4.8 V	6.0 V	7.4 V
Maximum current efficiency	9.9 cd/A	12.4 cd/A	11.5 cd/A	0.8 cd/A	7.2 cd/A
Maximum External Quantum Efficiency	11.8 %	14.8 %	13.6 %	12.8 %	8.6 %
CIE (x, y) (@ 1000 cd/m2)	0.66, 0.33	0.66, 0.33	0.66, 0.33	0.66, 0.33	0.66, 0.33

Table 4. Summary of performances of multiple quantum well red PHOLEDs in this study

4. Two layers structure

4.1 Introduction

Performance and efficiencies of red PHOLEDs devices have been improved in recent days, particularly in p-i-n type OLEDs (J. Huang et al., 2002; Pfeiffer et al., 2002). Good charge balance in emitting layers and low barrier to charge carriers injection in p-i-n devices demonstrate a low operating voltage and high efficiency. CBP is the most widely used host material in red and green emitting PHOLEDs (Chin et al., 2005; Tsuzuki, and Tokito , 2007). Other host materials such as 4,4',4"-tris(N-carbazolyl)-triphenylamine (TCTA), 3-phenyl-4-(1'-naphthyl)-5-phenyl-1,2,4-triazole (TAZ), 1,3,5-tris(N-phenylbenzimidizol-2yl)benzene (TPBI) and aluminum (III) bis(2-methyl-8-quinolinato)-4-phenylphenolate (BAlq) for PHOLEDs are also commercially available and used as a matter of convenience for many guest–host applications (Zhou et al., 2003; Che et al., 2006; J. H. Kim et al., 2003). HOMO , LUMO and triplet energy of these host materials are listed in Table 5. The HOMO and LUMO energy levels of bis(10-hydroxybenzo [h] quinolinato)beryllium complex ($Bebq_2$) are reported at 5.5 and 2.8 eV, respectively (S. W. Liu et al. 2004). High luminance in OLEDs with $Bebq_2$ as an emitter was reported by Hamada et al. (Hamada et al., 1993). Since $Bebq_2$ and beryllium complexes have very good electron transporting characteristics with high electron mobility of ~10^{-4} cm^2/Vs (Y. Liu et al., 2001; Vanslyke et al., 1991; J.-H. Lee et al., 2005) and narrow band gap, $Bebq_2$ can make a suitable candidate for the host of red emitting PHOLEDs (Jeon et al., 2008a, 2008b; Jeon et al., 2009; Pode et al., 2009).

Compounds	HOMO (eV)	LUMO (eV)	Reported Triplet Energy (eV)	Calculated Triplet Energy (eV)
CBP	5.8	2.5	2.6	2.8
TCTA	5.9	2.7	2.8	2.7
TPBI	6.3	2.8	…..	2.8
BAlq	5.9	3.0	2.2	2.6
TAZ	6.6	2.6	….	3.3
$Bebq_2$	5.5	2.8	….	2.5

Table 5. HOMO, LUMO and triplet energy levels of some fluorescent host materials for PHOLEDs

In this section, we report a narrow band gap electron transporting host material, $Bebq_2$, for red light-emitting PHOLEDs. The triplet energy of $Bebq_2$ host was estimated using density functional theory (DFT). Simple bi-layered PHOLEDs, tris(1-phenylisoquinoline)iridium ($Ir(piq)_3$) doped in $Bebq_2$ host, were fabricated and studied.

4.2 Experimental

Beryllium compound has been reported to have a strong fluorescence characteristic. Although long-lived phosphorescence, caused by spin-forbidden decay from the first triplet state (T_1), is a ubiquitous property of organic molecules, no report about the estimation of triplet energy of $Bebq_2$ host and its role on the device performance has been available to date. Therefore to estimate the triplet state energy, the phosphorescent spectrum of $Bebq_2$ was investigated at low temperature. However, no signature of phosphorescent peak in $Bebq_2$ complex is observed at 77 K. It only exhibits a strong fluorescence emission at 466 nm. Therefore, the molecular simulation method was employed to deduce the triplet energy of $Bebq_2$.

The triplet energy state, estimated by molecular modeling and DFT using DMoL3 program (version 4.2), was found to be about 3.0 eV (Park et al., 2008). Usually in phosphorescent host materials, singlet and triplet exchange energy value is about 0.5 eV. However, $Bebq_2$ host shows a very small exchange energy value of 0.2 eV and is a signature of strong electron-electron correlation. Triplet phosphorescent dopants such as $Ir(piq)_3$ and bis(2-phenylquinoline)(acetylacetonate)iridium ($Ir(phq)_2acac$), used in red light-emitting PHOLEDs, have triplet energy states (actual LUMO level) at 2.8 and 3.1 eV, respectively (Chin et al., 2005; T.-H. Kim et al., 2006). This triplet energy of dopant is very close to the triplet energy of the $Bebq_2$ host material, thus facilitating the electron movement in emitting layer.
Furthermore, corroboration of triplet energy state of $Bebq_2$ host and possible energy transfer from the host to dopant were confirmed by fluorescent and phosphorescent quenching experiments using iridium dopants and $Bebq_2$ host in tetrahydrofuran solution. The $Bebq_2$ fluorescence peak is efficiently quenched by $Ir(piq)_3$ dopant, transferring all its singlet energy directly to the dopant triplet state. As a consequence, we conclude that the triplet energy level of $Bebq_2$ is lower than that of the $Ir(piq)_3$ dopant and exchange energy of host material between singlet and triplet must be very small. However, the reported triplet energy value of ($Ir(piq)_3$) in Ref 63 is 2.8 eV which is lower than that of the $Bebq_2$ host (3.0 eV). So, the LUMO energy level (i.e. triplet state) of $Ir(piq)_3$ dopant was confirmed by the optical band-gap and cyclic voltametry measurements and was found to be 3.1 eV. Both host and dopant molecules seem to have almost same value of triplet energy.

4.3 Results & discussion

Figure 7 shows the structures of three red PHOLEDs devices fabricated for the present study. Devices A and B have a conventional multilayer structure containing hole and electron transport and injection, and hole blocking layers with CBP and $Bebq_2$ host materials, respectively. Device A with a CBP host material is used as a control device, while the fabricated device C with $Bebq_2$ host has a simple bilayered structure. Red phosphorescent OLEDs were fabricated as follows:
Devices A & B: ITO / α-NPB (40 nm) / HOST : Dopant (10 wt%, 30 nm) / Balq (5 nm) / Alq_3 (20 nm) / LiF(0.5 nm) / Al(100 nm), and Device C: ITO/α-NPB (40 nm) / HOST : Dopant (10 wt%, 50 nm)/ LiF(0.5 nm) / Al(100 nm)

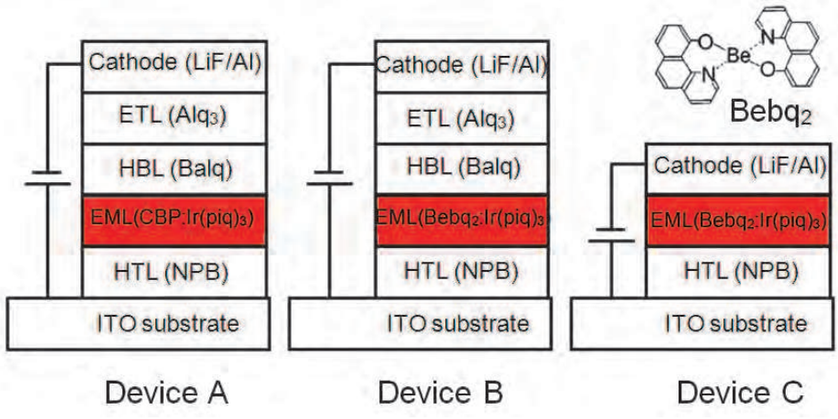

Fig. 7. Structures of fabricated three PHOLEDs: device A - CBP: $Ir(piq)_3$, device B - $Bebq_2$: $Ir(piq)_3$, device C - $Bebq_2$: $Ir(piq)_3$ without HBL and ETL.

Figure 8 shows the I-V-L characteristics of fabricated red phosphorescent devices. At a given constant voltage of 5 V, current density values of 0.82, 2.83, and 18.99 mA/cm² in the fabricated devices A, B, and C are noticed as displayed in Fig. 8, respectively. The driving voltage for the device A to reach 1000 cd/m² is 8.8 V, 6.8 V for the device B, and 4.5 V for the device C. A low turn-on voltage of 4.5 V in device C with a simple bi-layered structure compared to control device A with CBP host (8.8 V), is observed. The resistance to current conduction in bilayered device C is significantly reduced. As the HOMO energy of $Bebq_2$ host is at 5.5 eV, holes injected from the hole transport layer (HTL) trap directly at the

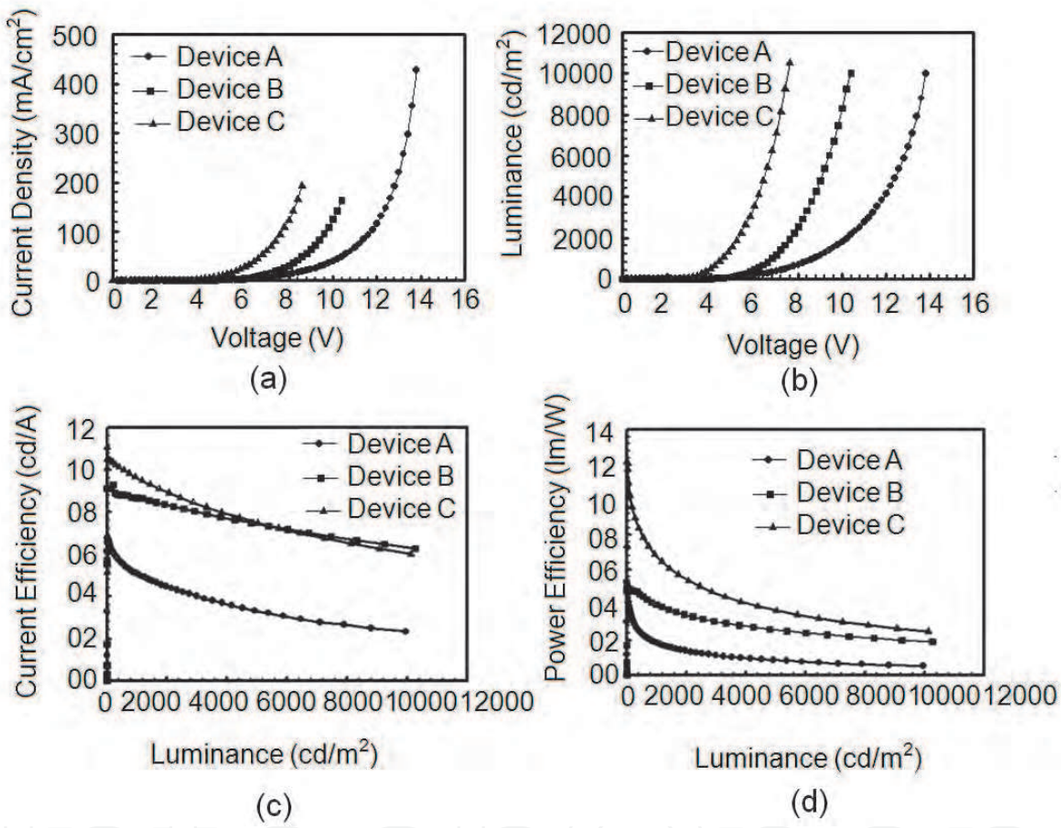

Fig. 8. I-V-L characteristics of fabricated three PHOLEDs ; (a) current-voltage characteristics (b) luminance-voltage characteristics (c) current efficiency-luminance (d) power efficiency luminance.

HOMO level (5.1 eV) of dopant. Barrier to hole injection in the device C is almost negligible. Also, electrons injected from the cathode move freely in the emitting layer as the LUMO (triplet) of dopant and triplet of host are at the same energy and finally captured at the trapped hole sites giving rise to phosphorescent emission. Multilayer structure as displayed in devices A and B introduces heterobarriers to electron and hole injection into emitting layers, thus enhancing the turn-on voltages, although some reduction of driving voltage in device B due to narrow band gap $Bebq_2$ host materials is noticed. Moreover in CBP based PHOLEDs, severe charge trapping at NPB interface has been reported by several researchers [63, 64]. Figure 9 shows the energy band diagram of device C. The current and power efficiency characteristics of fabricated devices are shown in Fig. 8 (c) & (d). At a given

constant luminance of 1000 cd/m², the current and power efficiencies are 9.66 cd/A and 6.90 lm/W for the device C, 8.67 cd/A and 4.00 lm/W for the device B, and 5.05 cd/A and 1.80 lm/W for the device A, respectively. These values of device C are improved by a factor of 1.9 and 3.8 times compared with those of device A, respectively. In device reliability tests, device A and C show very different behaviors. Device A shows about 120 h lifetime at 1000 nit, while lifetime of 150-160 h is noticed in $Bebq_2$ device. Relatively small initial decrease of brightness value and gradual decay curve is observed in device C, which indicates $Bebq_2$ device reliability is relatively very good. However, material stability of $Bebq_2$ seems not to be good. Figure 10 shows the electroluminescence spectra at a brightness of 1000 cd/m² of different fabricated phosphorescent red-emitting devices. Clean red light emission at 632 nm observed in device C indicates the complete energy transfer from a novel narrow band gap $Bebq_2$ host material to $Ir(piq)_3$ dopant. The CIE coordinate of three red devices show the same coordinate as CIE (0.67, 0.33).

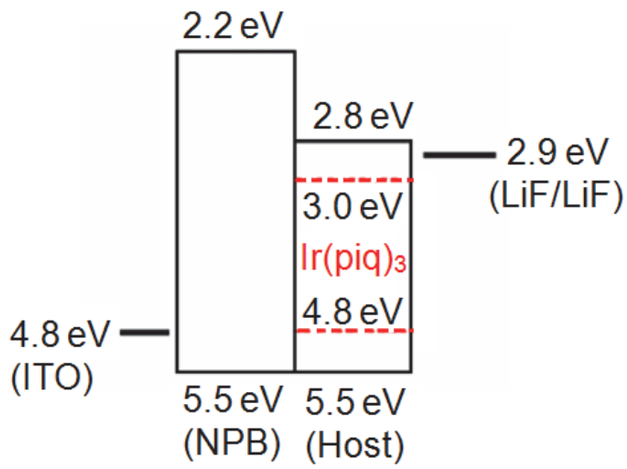

Fig. 9. Energy diagram of red organic bi-layered PHOLEDs with $Bebq_2$:$Ir(piq)_3$ host (Device C).

Anyway, interesting and intriguing results on the performance of bi-layered device C have been obtained. The LUMO level of $Bebq_2$ material (2.8 eV), very close to LUMO values of Balq, Alq_3 and LiF cathode, offers almost no barrier to electron injection between the emitting layer and LiF cathode. Furthermore, excellent electron transporting property of $Bebq_2$ material favors to mobility of electrons which provides a good charge balance in the emitting layer. HOMO levels of $Bebq_2$ host and NPB hole transport layer in the fabricated device C are very close while LUMO energy levels of host and dopant are almost same. Therefore, the emission process in PHOLEDs device C via electron trapping at LUMO and hole trapping at HOMO seems to be minimized, giving to low driving voltage value. In this device C, the emission of red light may be originated from the direct electron capturing from the host and recombining at holes trapped at the HOMO of the dopant in the emitting layer. Indeed, the hole trapping in bilayered device C is not a serious issue. To investigate the influence of recombination zone position on the emission and hole trapping, three PHOLEDs with emitting zone at X = 0, 10, and 20 nm from the HTL/EML interface were fabricated and studied as displayed in Table 6 and Fig. 11. Results reveal excellent emission of red light in all devices, except some contribution to the emission from the $Bebq_2$ host material in devices with X = 10 and 20 nm. These results demonstrate that the emission zone in simple bilayered

PHOLEDs is very broad and hole trapping is not so severe. The EL emission spectra of devices D, E, and F are shown in Fig. 12(a) and CIE coordinates in Fig. 12(b).

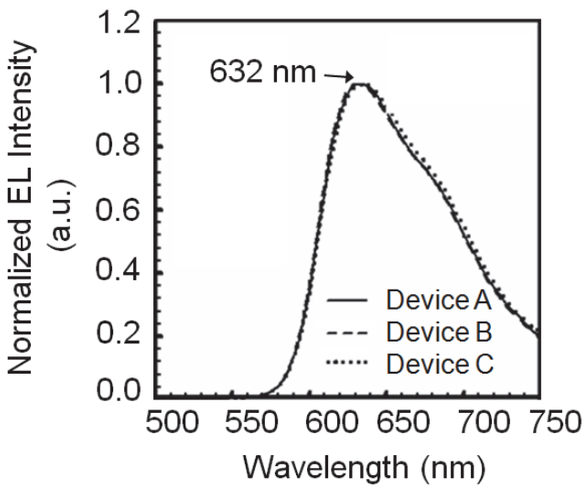

Fig. 10. Normalized electroluminescent spectra of devices A, B, and C at the luminance of 1000 cd/m^2.

Thickness (Å)	Device D	Device E	Device F
X (nm)	0	10	20
$Bebq_2$:$Ir(piq)_3$	100	100	100
$Bebq_2$	400	300	200

Table 6. Recombination zone position in Device C from the HTL/EML interface

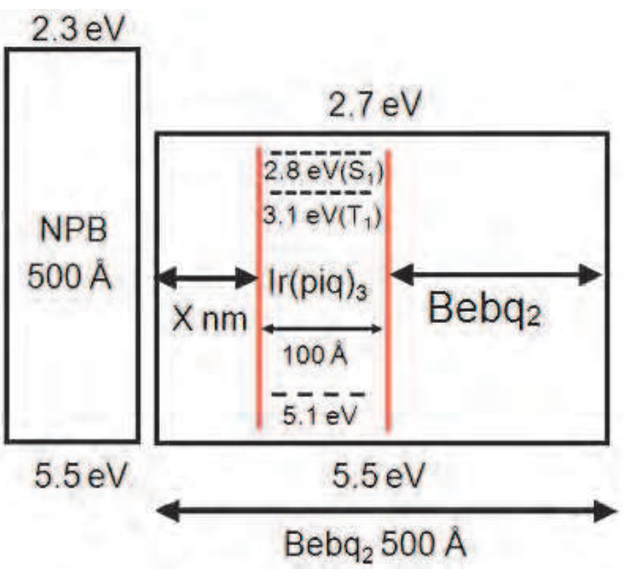

Fig. 11. Recombination zone position in Device C

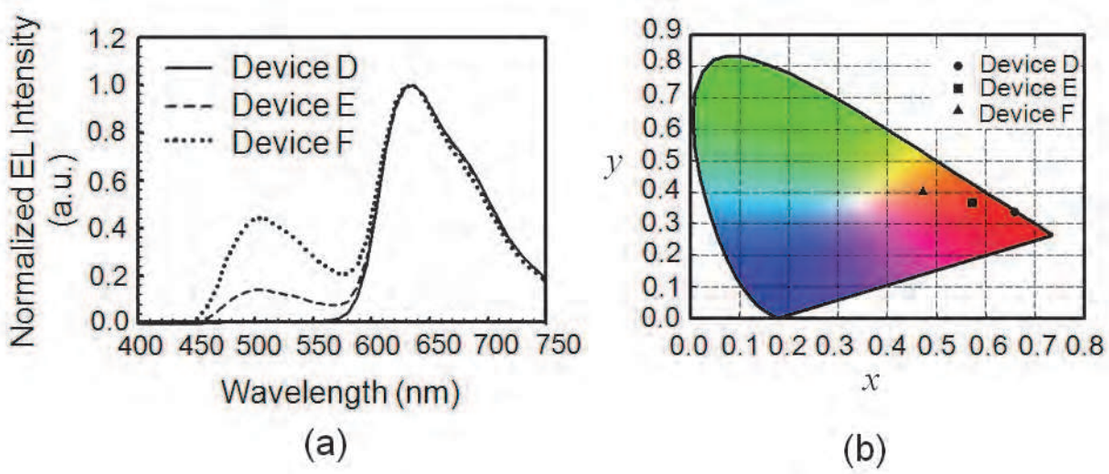

Fig. 12. (a) EL emission spectra, and (b) CIE coordinates of devices D, E, and F.

4.2 Conclusions

A narrow band-gap host material, $Bebq_2$, for red PHOLEDs with a very small exchange energy value of 0.2 eV between singlet and triplet states has been demonstrated. It shows almost no barrier to injection of charge carriers and charge trapping issue in PHOLEDs is minimized. High current and power efficiency values of 9.66 cd/A and 6.90 lm/W in bi-layered simple structure PHOLEDs are obtained, respectively. The operating voltage of bi-layered PHOLEDs at a luminance of 1000 cd/m^2 was 4.5 V. In conclusion, simple bilayerd red emitting device with $Bebq_2$ host could be a promising way to achieve efficient, economical, and ease manufacturing process, important for display and lighting production.

5. Single layer structure

5.1 Introduction

Organic light emitting devices (OLEDs) have made significant stride (Pfeiffer et al., 2002) and the technology has already been commercialized to mobile flat panel display applications. Thermal evaporation technique and complicated fabrication process consisting of multiple layers for charge carriers balancing and exciton confinement (Baldo and Forrest, 2002; Coushi et al., 2004; Tanaka et al., 2007) are employed in highly efficient phosphorescent OLEDs. In order to overcome such complex device architecture, many good approaches are enduring until now. High efficiency devices with pure organic bilayered OLEDs have been reported by several researchers (Jeon et al., 2008b; Pode et al., 2009; Park et al., 2008; Meyer et al., 2007; Z. W. Liu et al., 2009). Furthermore, bilayered devices consisting of an organic single layer with a buffer layer on the electrode have also been reported without any significant improvement of the device performances (Q. Huang et al., 2002; Gao et al., 2003; Wang et al., 2006; Tse et al., 2007). However, truly organic single layered approach is almost rare. To date, only an exclusive article on the red emitting PHOLED single layer device with a tris[1-phenylisoqunolinato-C2,N]iridium (III) ($Ir(piq)_3$) (21 wt%) doped in TPBi (100 nm) with low values of current and power efficiencies under 3.7 cd/A and 3.2 lm/W at 1 cd/m^2 have been reported, respectively (Z. Liu et al., 2009).

In this section, we have presented efficient and simple red PHOLEDs with only single organic layer using thermal evaporation technique. The key to the simplification is the direct

injection of holes and electrons into the mixed host materials through electrodes. In conventional OLEDs, usually the Fermi energy gap between cathode (~ 2.9 eV) and surface treated anode (~ 5.1 eV) is about 2.0~2.2 eV which is close to the red light emission energy (1.9 ~2.0 eV). As a consequence, red devices do not at all require any charge injection and transporter layer if the host material has proper HOMO and LUMO energy levels. However, such host materials are very rare. The most suitable option to address such issues is to employ the mixed host system to adequately match the energy levels between emitting host and electrodes. Mixed host system of electron and hole transporting materials to inject electrons and holes from electrodes into the organic layer without any barrier has been studied, respectively and employed for the charge balance. Thus, hole type host materials are required to have HOMO energy levels at 5.1~5.4 eV to match with the Fermi energy of surface treated ITO (5.1 eV). While 2.8~3.0 eV LUMO energy levels of electron transporting host materials are necessary to match the Fermi level of cathode. 4,4′,4″-Tris(N-3-methylphenyl-N-phenyl-amino)triphenylamine(m-MTDATA) and N,N′-diphenyl-N,N′-bis(1,1′-biphenyl)-4,4′-diamine (α-NPB) were used as the hole transporting host materials. Bis(10-hydroxybenzo[h]quinolinato)beryllium ($Bebq_2$) with 2.8 eV LUMO energy was used as the electron transport host material and $Ir(piq)_3$ was employed as a red phosphorescent guest.

5.2 Experimental

m-MTDATA and α-NPB as hole transporting host materials, $Bebq_2$ as an electron transporting host material, and $Ir(piq)_3$ as a red dopant were obtained from Gracel Corporation. Details of the fabrication process have been discussed section 3. The emitting area of PHOLED was 2 mm^2 for all the samples studied in the present work.

5.3 Results & discussion

Figure 13 shows the energy band-diagram of the single layer red PHOLEDs used in the present work. For the evaluation of single layer with different mixed host systems, the following devices were fabricated:

Device A: ITO/m-MTDATA:$Bebq_2$: $Ir(piq)_3$ [1~4 wt%, 100 nm]/LiF (0.5 nm)/Al (100 nm), and Device B: ITO/α-NPB:$Bebq_2$: $Ir(piq)_3$ [1~4 wt%, 100 nm]/LiF (0.5 nm)/Al (100 nm).

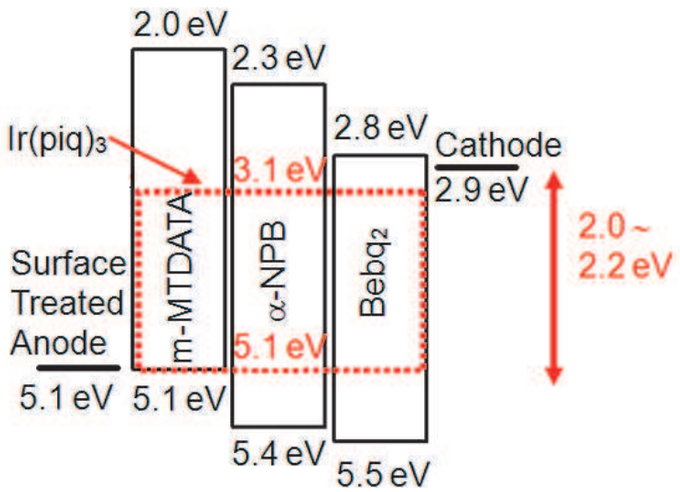

Fig. 13. Energy band-diagram of the single layer red PHOLEDs.

The ratio of the hole and electron transporting hosts was fixed to 1:1. The doping concentrations were varied from 1% to 4% to optimize the device performance. Table 7 shows the performance of red PHOLEDs devices comprising a single emitting layer. The current and power efficiencies values of 7.44 cd/A, and 3.43 lm/W at 1000 cd/m² brightness value are reported in 4wt% doped device A, respectively. The driving voltage (to reach 1000 cd/m²) is 6.9 V. Very similar device performances are obtained in 2 wt% doped device A. The optimum doping condition for Device A seems to be 4 wt% as the highest efficiency is observed at an acceptable brightness value (1000 cd/m²). Whereas, the driving voltage, current and power efficiencies values of 5.4 V, 9.02 cd/A, and 5.25 lm/W at brightness value of 1000 cd/m² are reported in device B with 1 wt% of optimum doping condition, respectively. Maximum current efficiency values for devices A and B were appeared in 4 and 1 wt% of $Ir(piq)_3$ doped mixed hosts, respectively. The color coordinates are (0.66, 0.33) or (0.67, 0.32) for all devices. Even in 1% doped device, a good red emission color is observed.

	Device A			Device B		
	1% Doping	2% Doping	4% Doping	1% Doping	2% Doping	4% Doping
Turn on voltage (@ 1cd/m²)	2.5 V	2.4 V	2.3 V	2.4 V	2.4 V	2.4V
Operating voltage (@ 1000 cd/m²)	7.2 V	7.1 V	6.9 V	5.4 V	5.4 V	5.3 V
Maximum current and power efficiency	8.12 cd/A 7.84 lm/W	8.19 cd/A 9.86 lm/W	8.04 cd/A 10.96 lm/W	9.44 cd/A 10.62 lm/W	8.36 cd/A 9.82 lm/W	7.04 cd/A 8.11 lm/W
current and power efficiency (@ 1000 cd/m²)	7.28 cd/A 3.18 lm/W	7.34 cd/A 3.29 lm/W	7.44 cd/A 3.43 lm/W	9.02 cd/A 5.25 lm/W	8.26 cd/A 4.80 lm/W	7.04 cd/A 4.10 lm/W
CIE (x, y) (@ 1000 cd/m²)	(0.66, 0.33)	(0.67, 0.32)	(0.67, 0.32)	(0.66, 0.33)	(0.67, 0.32)	(0.67, 0.32)

Table 7. Device performances of various single red devices with different doping concentration

The results of device B (1wt %) is significantly superior to $Ir(piq)_3$ doped multi-layer red PHOLEDs [73]. Device B shows that the doping concentration in PHOLEDs can be reduced until 1~2% range with higher efficiency provided HOMO-HOMO and LUMO-LUMO differences between host and dopant molecules are within ~0.3 eV and emission zone is within 50nm. Device B displays exactly similar behavior although the HOMO-HOMO gap is relatively higher as compared to that in device A. However, unlike device B, similar device properties in device A regardless of doping condition from 1 to 4% are obtained. The self

quenching by dopants seems to be not so serious in this device A. This indicates that the emission zone of device A is very broad and the charge balance is also relatively poor. The efficiency of device A is low compared to device B, but 4% doped condition in device A has a little better charge balance.

The J-V-L curve and efficiency characteristics of devices A and B are shown in Fig. 14. The best efficiency yields of 9.44 cd/A (EQE 14.6%) and 10.62 lm/W are noticed in the device B as shown in Fig 14(b). As seen from the results of Fig. 14(a), the driving voltage in device A with m-MTDATA:Bebq$_2$:Ir(piq)$_3$ [4 wt%] is 6.9 V at the brightness of 1,000 cd/m^2. The device B with α-NPB:Bebq$_2$:Ir(piq)$_3$ [1 wt%] shows a driving voltage of 5.4 V at 1000 cd/m^2.

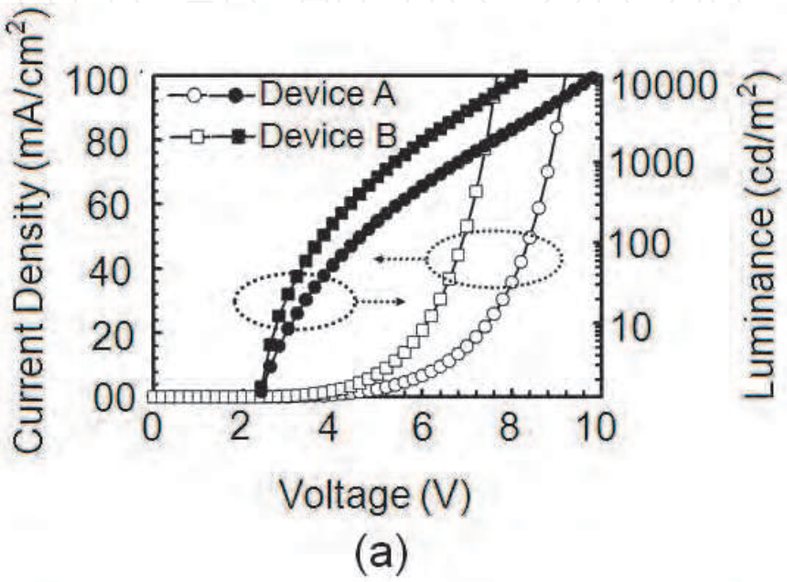

Fig. 14. Current density (J)-Voltage(V)-Luminance (L) and Efficiency characteristics of single layer red PHOLEDs. (a) J-V-L characteristics, (b) L vs. current and power efficiencies characteristics. Device A(4%) and Device B(1%) fully doped.

In m-MTDATA, no barrier for hole injection from the surface treated ITO (5.1 eV) to the HOMO (5.1 eV) of the m-MTDATA exists. Further, this energy level matches with the HOMO (5.1 eV) of the $Ir(piq)_3$. While, electrons injected from the cathode move freely on the LUMO energy of $Bebq_2$. In case of the device B, the HOMO energy in the α-NPB material at 5.4 eV as against 5.1 eV in the surface treated ITO (HOMO difference ~ 0.3 eV) offers some barrier to the hole injection into the emitting layer. While electrons injected from cathode move freely over the LUMO energy of $Bebq_2$. *To understand the injection barrier situation in m-MTDATA and a-NPB, J-V of hole only devices were investigated*. An ideal Ohmic contact (Giebeler et al., 1998) at ITO and m-MTDATA interface was reported. Whereas, the NPB hole only device had reported to have the injection limited current behavior. When a buffer layer like PEDOT:PSS (poly(3,4-ethylenedioxythiophene)-poly(4-stylenesurfonate) or C60 was introduced at ITO interface, the Ohmic characteristic was observed in this device (Tse et al., 2006; Koo et al., 2008). Form these previously reported results, a high value of driving voltage in the α-NPB mixed device B due to the high barrier to hole injection into the emitting layer was expected. However in reality, the device B with α-NPB hole transporting host shows a lower driving voltage implying a low resistance to the current flow. Here, devices A and B were realized using two different hole transporting host materials having different charge carriers transport abilities, particularly the hole mobility. α-NPB has an ambipolar transporting ability with the hole mobility faster than that of m-MTDATA (S. W. Liu et al., 2007). Thus, mobilities of hole carriers in these mixed host single layer systems rather than hole injection barrier at the ITO/mixed host interface seems to be crucial in deciding the driving voltage. In order to elucidate the conduction and emission processes in single layer devices, we have fabricated following several devices and investigated.

We have made devices C and D without $Ir(piq)_3$ dopant and results were compared with those of devices A and B, respectively. Fig. 15 shows J-V characteristics of devices A,B,C,D. Results on bi-layered ITO/α-NPB (40 nm) / $Bebq_2$: $Ir(piq)_3$ (10 wt%, 50 nm) /LiF (0.5 nm) /Al(100 nm) red emitting PHOLEDs [73], reproduced here for better comparison, show a low driving voltage value of 4.5 V to reach a luminance of 1000 cd/m^2. As displayed in Fig. 15, both devices C and D (undoped) show J-V characteristics similar to $Ir(piq)_3$ doped devices A and B, respectively. Furthermore in our devices A and B, hole and electron injection barriers by dopant molecules are negligible due to no barrier at ITO and cathode interfaces, respectively. Doping in the device may affect carrier mobility due to carrier trapping by dopant molecules. Usually, J-V characteristics of PHOLEDs are changed significantly by adding dopant molecules when HOMO-HOMO and LUMO-LUMO differences between host and dopant molecules are high over 0.3 eV. In device C and D, these energy differences are within 0.3 eV. In this case, the J-V characteristic does not change because trapped charges in dopant molecules easily overcome to host energy level by thermal energy. Described results demonstrate that the conduction of current in a hole and electron transporting mixed host layer is almost independent of (i) the charge trapping at dopant molecules and (ii) hole injection barrier at the ITO/mixed host interface. Further, all mixed single layer devices offer a high resistance to current flow than bi-layered red device with hetero junction (see Fig. 15). The interesting and intriguing results on J-V in mixed host single layer devices may be explained on the basis of existing knowledge on carrier mobilities in organic materials. α-NPB exhibits an ambipolar transporting ability with electron and hole mobility values of 9×10^{-4} and 6×10^{-4} cm^2/Vs, respectively (S. W. Liu et al., 2007), while the hole mobility value in m-MTDATA

is 3×10^{-5} cm²/Vs. Earlier, it was shown that the charge transport behaviors in mixed thin films of α-NPB and Alq_3 are sensitive to (i) compositional fraction, and (ii) charge carriers mobilities of neat compounds (S. W. Liu et al., 2007). The 1:1 mixed layer of α-NPB and Alq_3 appeared to give lower charge carrier mobility of 10^{-2}~10^{-3} order than neat films (S. W. Liu et al., 2007). As a consequence, the fast current flow in the device B despite the large hole injection barrier is attributed to the high hole mobility value and ambipolar nature of α-NPB. Higher driving voltage of single layer devices compared to the bilayer device is also well understood by the decrease in carrier mobility in the mixed host system.

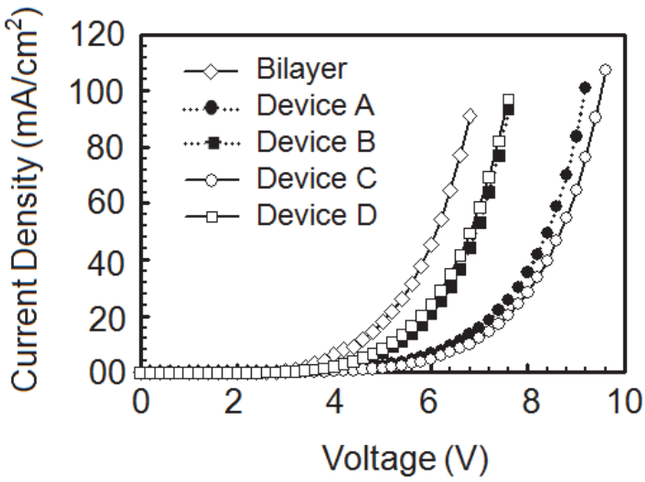

Bilayered device: ITO/α-NPB (40 nm) / $Bebq_2$: $Ir(piq)_3$ (10 wt%, 50 nm) /LiF (0.5 nm)/Al(100 nm); Device A: ITO/m-MTDATA:$Bebq_2$: $Ir(piq)_3$ [4 wt%, 100 nm]/LiF (0.5 nm)/Al (100 nm); Device B: ITO/α-NPB:$Bebq_2$: $Ir(piq)_3$ [1 wt%, 100 nm]/LiF (0.5 nm)/Al (100 nm); Device C: ITO/m-MTDATA:$Bebq_2$ [100 nm]/LiF (0.5 nm)/Al (100 nm); Device D: ITO/α-NPB:$Bebq_2$ [100 nm]/LiF (0.5 nm)/Al (100 nm)

Fig. 15. J-V characteristics of bi-layered and A~D red emitting PHOLEDs devices.

Since the charge transport behaviors in mixed hosts are sensitive to the composition and intrinsic mobilities in neat films, the location of the recombination region may be important to understand the device efficiency. To investigate the recombination zone position, we have evaluated three devices with doped emissive layer located at different positions as:

1. Device A-(L) : ITO/m-MTDATA:$Bebq_2$:$Ir(piq)_3$ [4 wt%, 30 nm]/m-MTDATA:$Bebq_2$ [70 nm]/LiF (0.5 nm)/Al (100 nm);
2. Device A-(C) : ITO/m-MTDATA:$Bebq_2$ [35 nm]/m-MTDATA:$Bebq_2$:$Ir(piq)_3$ [4 wt%, 30 nm]/m-MTDATA:$Bebq_2$ [35 nm]/LiF (0.5 nm)/Al (100 nm);
3. Device A-(R) : ITO/m-MTDATA:$Bebq_2$ [30 nm]/m-MTDATA:$Bebq_2$:$Ir(piq)_3$ [4 wt%, 70 nm]/LiF (0.5 nm)/Al (100 nm).

Similarly, Devices B-(L), (C) and (R) were fabricated using α-NPB instead of m-MTDATA and 1 wt% of $Ir(piq)_3$. The doping region was fixed to 30 nm in all devices. The anode side doped devices show the best current efficiency performance as displayed in Fig. 16 (Devices A-(L) and B-(L)), indicating that the recombination zone is around the ITO/mixed host interface. Further, the emission efficiency performance deteriorates as the

doped region is moved toward the cathode side. High current efficiency in α-NPB/$Bebq_2$ mixed host system is the consequences of the better charge balance in the recombination zone. Figure 17 shows electroluminescence (EL) spectra dependence on the emission zone location in doped and undoped devices. Broad and clean EL peak at 620 nm in undoped mixed m-MTDATA/$Bebq_2$ host organic device C is due to exciplex emissions. While the strong and asymmetric EL emission peak at 620 in devices A- (L) to A- (R) due to emissions of exciplex and $Ir(piq)_3$ red phosphorescent dopant are noticed. In these devices, exciplexes are formed as the energy difference between HOMO of m-MTDATA and LUMO of $Bebq_2$ is about 2.3 eV. Whereas in case of fully doped (device B) and undoped (device D) α-NPB/$Bebq_2$ mixed devices, clean peaks at 510 and 620 nm due to strong emission of $Bebq_2$ and $Ir(piq)_3$ dopant are appeared, respectively. Upon moving the doped region toward the anode side, EL spectra show both emission peaks at 510 and 620 nm due to $Bebq_2$ host and $Ir(piq)_3$ dopant, respectively, but with the reduced intensity of 510 nm emission peak of $Bebq_2$. The electron charge carriers are transported over the LUMO of $Bebq_2$ through the doped region and reach the anode side, resulting in the emission due to $Bebq_2$ host.

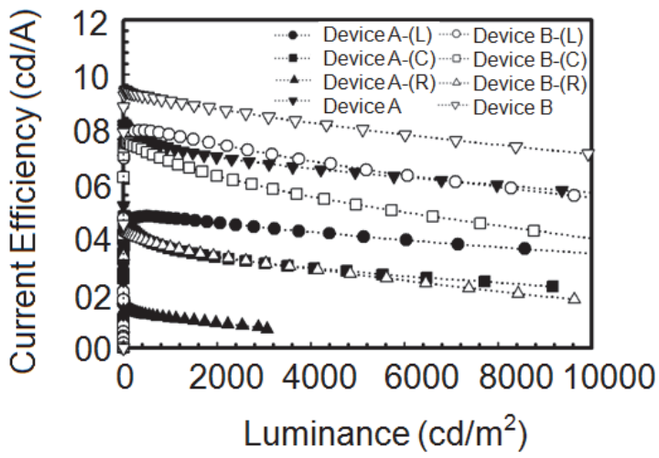

Fig. 16. Luminance-current Efficiency characteristics of various single layer devices fabricated with different locations of doped regions. Device A – Fully doped, Device B- Fully doped.

Device A: ITO/m-MTDATA:$Bebq_2$: $Ir(piq)_3$ [4 wt%, 100 nm]/LiF (0.5 nm)/Al (100 nm) – Fully doped; Device C: undoped mixed m-MTDATA/$Bebq_2$ organic host device
Device B: ITO/α-NPB:$Bebq_2$: $Ir(piq)_3$ [1 wt%, 100 nm]/LiF (0.5 nm)/Al (100 nm)- Fully doped; Device D: undoped mixed α-NPB:$Bebq_2$ organic host device
Although holes are easily injected into the m-MTDATA/$Bebq_2$ organic layer (device A), they are slowly transported due to low hole mobility in m-MTDATA which is further reduced in the mixed host system. While transport behavior in α-NPB/$Bebq_2$ mixed host system is relatively better due to the high hole mobility in α-NPB. Whereas, electrons in both doped devices A and B are transported freely over the LUMO of the $Bebq_2$. These results corroborate that the recombination zone in devices A and B are located between the anode and the center of the emitting layer.

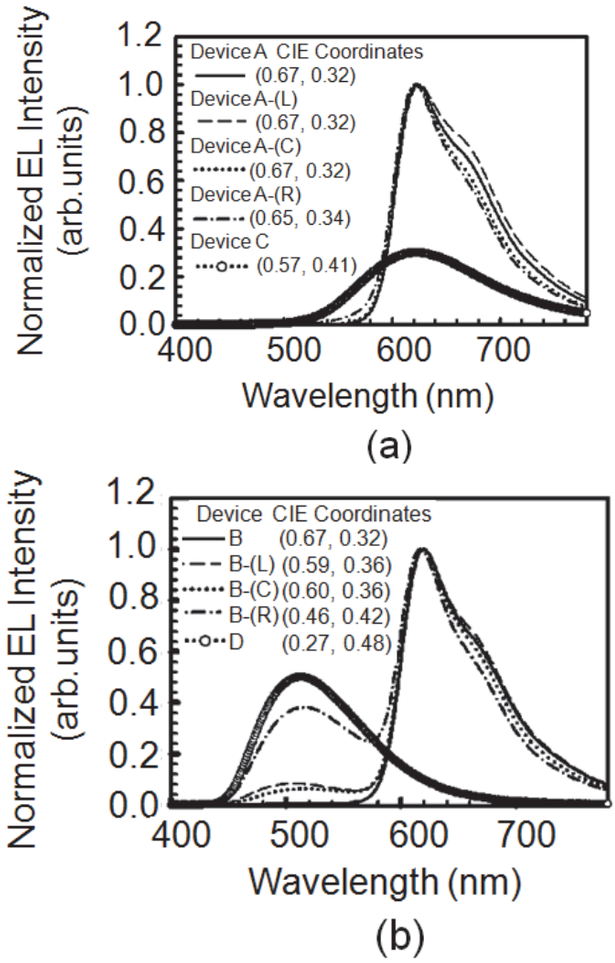

Fig. 17. Electroluminescence (EL) spectra of various single layer devices fabricated with different locations of doped regions at the brightness of 1000 cd/m².

5.4 Conclusions

In conclusion, we have demonstrated high efficiency red PHOLEDs comprising only single emitting layer. The key to the simplification is the direct injection of holes and electrons into the mixed host materials through electrodes. The driving voltage of 5.4 V to reach the 1000 cd/m² and maximum current and power efficiency values of 9.44 cd/A and 10.62 lm/W, respectively, in the α-NPB/ $Bebq_2$ mixed single layer structure PHOLEDs with the $Ir(piq)_3$ dopant as low as 1 wt% are obtained. We found that carrier mobility is significantly important parameter to simplify the device architecture. The obtained characteristics of red PHOLEDs pave the way to simplify the device structure with reasonable reduction in the manufacturing cost of passive and active matrix OLEDs.

6. Ideal host and guest system

6.1 Introduction

In phosphorescent devices, theoretically 100% internal quantum efficiency (IQE) is achieved by harvesting both singlet and triplet excitons generated by electrical injection which is four

times that of fluorescent organic light-emitting devices (OLEDs) (Gong et al., 2002; Tsuzuki et al., 2003; Adachi et al., 2000). Förster and/or Dexter energy transfer processes (Tanaka and Tokito, 2008) between host and guest molecules play an important role in confining the triplet energy excitons in the phosphorescent guest. This determines the triplet state emission efficiency in PHOLEDs. Förster energy transfer (Forster, 1959) is a long range process (up to ~ 10 nm) due to dipole-dipole coupling of donor host and acceptor guest molecules, while Dexter energy transfer (Dexter, 1953) is a short range process (typically ~ 1 to 3 nm) which requires overlapping of the molecular orbital of adjacent molecules (intermolecular electron exchange).

The phosphorescence emission in the conventional host-guest phosphorescent system occurs either with Förster transfer from the excited triplet S_1 state of the host to the excited triplet S_1 state of the guest and Dexter transfer from the excited triplet T_1 state of the host to the excited triplet T_1 state of the guest or direct exciton formation on the phosphorescent guest molecules, resulting in a reasonable good efficiency. However, emission mechanism in phosphorescent OLEDs whether due to charge trapping by guest molecules and/or energy transfer from the host to the guest, is not clearly understood. Till date, several researchers have reported that the charge trapping at guest molecules is the main cause for the emission of PHOLEDs.

Amongst well-known iridium (III) and platinum (II) phosphorescent emitters, Iridium (III) complexes have been shown to be the most efficient triplet dopants employed in highly efficient PHOLEDs (Adachi et al., 2001b; Baldo et al., 1999). Usually, wide energy gap 4,4'-bis(N-carbazolyl)-1,1'-biphenyl (CBP) is used as a host material for red (~ 2.0 eV) or green (~ 2.3 – 2.4 eV) phosphorescent guests [63, 64]. Such a wide energy gap host has the advantage of high T_1 energy of 2.6 eV (Baldo & Forrest, 2000) or 2.55 eV (Tanaka et al., 2004) and long triplet lifetime > 1 *s* (Baldo & Forrest, 2000), while the optical band gap value (E_g) is 3.1 eV (Baldo et al., 1999).

Fig. 18(a) shows both the energy level diagram of *fac*-tris(2-phenyl-pyridinato)iridium(III) ($Ir(ppy)_3$) green and the tris(1-phenylisoquinoline)iridium ($Ir(piq)_3$) red phosphorescent complexes used in doping the CPB host. However, the wide band gap host and narrow band gap (E_g) guest system often causes an increase in driving voltage due to the difference in HOMO and/or LUMO levels between the guest and host materials (Tsuzuki & Tokito, 2007). Thus, the guest molecules are thought to act as deep trapping centers for electrons and holes in the emitting layer, causing an increase in the drive voltage of the PHOLED (Gong et al., 2003). The dopant concentration in such a host-guest system is usually as high as about 6 ~ 10 percent by weight (wt%) because injected charges move through dopant molecules in the emitting layer. Therefore, self-quenching or triplet-triplet annihilation by dopant molecules is an inevitable problem in host-guest systems with high doping concentrations. Earlier, Kawamura et al. had reported that the phosphorescence photoluminescence quantum efficiency of $Ir(ppy)_3$ could be decreased by ~5% with an increasing in doping concentration from 2 to 6% (Kawamura et al., 2005). Consequently, the selection of suitable host candidates is a critical issue in fabricating high efficiency PHOLEDs.

In this section, the minimized charge trapped host-dopant system is investigated by using a narrow band-gap fluorescent host material in order to address device performance and manufacturing constraints. Here, we report an ideal host-guest system that requires only 1% guest doping condition for good energy transfer and provides ideal quantum efficiency in PHOLEDs. We also report that strong fluorescent host materials function very well in

phosphorescent OLEDs due to efficient Förster energy transfers from the host singlet state to the guest singlet and triplet mixing state which appears to be the key mechanism.

6.2 Experimental

N,N′-di(4-(N,N′-diphenyl-amino)phenyl)-N,N′-diphenylbenzidine (DNTPD) as a hole transporting layer, CBP and bis(10-hydroxybenzo [h] quinolinato)beryllium complex (Bebq2) as host materials, bis(2-phenylquinoline)(acetylacetonate)iridium (Ir(phq)2acac), tris(1-phenylisoquinoline)iridium (Ir(piq)3) as red dopants, aluminum (III) bis(2-methyl-8-quinolinato)-4-phenylphenolate (BAlq) as a hole blocking layer and Tris-(8-hydroxyquinoline)aluminum (Alq_3) as an electron transporting layer were purchased from Gracel and Chemipro Corporation and were used. The fabricated devices are characterized as described in the section 3. The OLED area was 2 mm^2 for all the samples studied in this work.

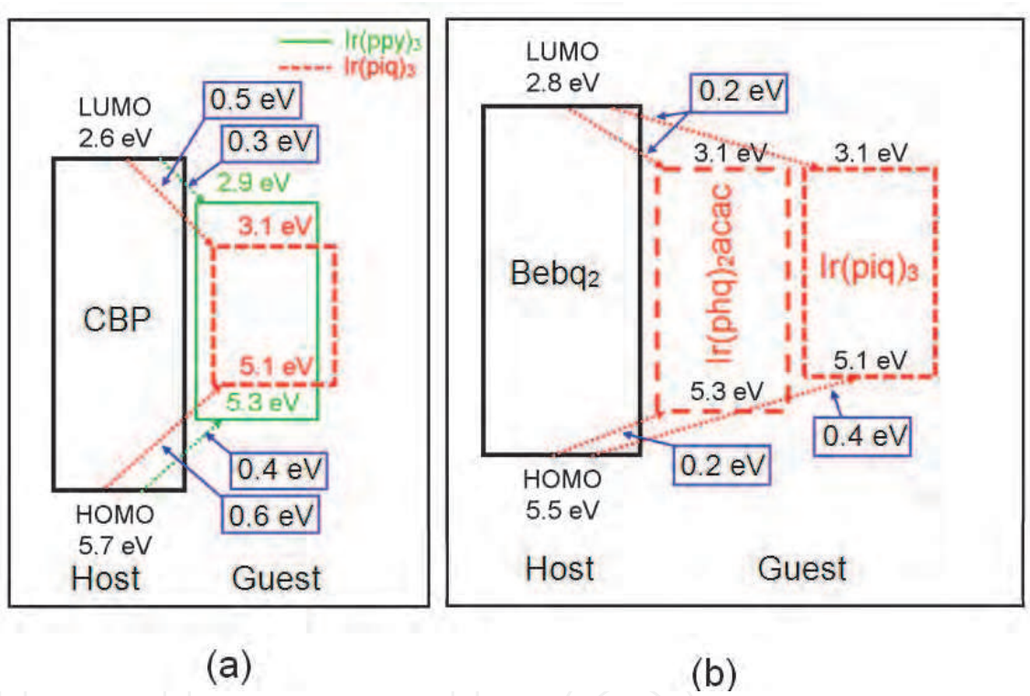

Fig. 18. (a) Energy level diagram of the $Ir(ppy)_3$ green and $Ir(piq)_3$ red phosphorescent complex doped by the CPB host. (b) Energy level diagram of the $Bebq_2$ fluorescent host and ($Ir(phq)_2acac$) and $Ir(piq)_3$ red phosphorescent dopant materials.

6.3 Results & discussion

Fig. 18(b) shows an energy band diagram of the fluorescent host and orange-red phosphorescent dopant materials used in the device fabrication. The simple bilayer PHOLED comprises a DNTPD hole transport layer (HTL), a $Bebq_2$ narrow band gap fluorescent host and an electron transport layer (ETL) plus $Ir(phq)_2acac$ dopant. In the present investigation, the fabricated PHOLED was:

ITO/DNTPD (40 nm) / $Bebq_2$: $Ir(phq)_2acac$ (50 nm, 1%)/ LiF(0.5 nm) / Al(100 nm).

Fig. 19 (a) & (b) and Table 8 (Device B) illustrate the electrical performance of the fabricated phosphorescent device. A luminance of 1000 cd/m^2 was obtained with a driving voltage of 3.7 V, and current and power efficiency values of 20.53 cd/A and 23.14 lm/W, respectively.

Furthermore, the maximum current and power efficiencies were 26.53 cd/A and 29.58 lm/W, respectively. The external quantum efficiency (EQE) value of 21% in the fabricated PHOLED slightly exceeded the theoretical limit of about 20% derived from simple classical optics. Moreover, this can be further improved by optimizing the output coupling. These remarkable results brought some pleasant surprises.

$Ir(phq)_2acac$ concentration (wt%)	Device A (0.5)	Device B (1.0)	Device C (1.5)	Device D (2.0)
Turn-on voltage (V) (at 1 cd/m²)	2.1	2.1	2.1	2.1
Operating voltage (V) (1000 cd/m²)	3.7	3.7	3.6	3.6
Efficiency (at 1000 cd/m²) Current (cd/A) Power (lm/W)	 20.96 18.29	 20.53 23.14	 22.61 19.73	 21.45 18.72
Maximum Efficiency Current (cd/A) Power (lm/W)	 21.25 24.62	 26.53 29.58	 23.46 29.94	 22.73 27.94
CIE (x,y) (1000 cd/m²)	(0.61,0.38)	(0.62,0.37)	(0.62,0.37)	(0.62,0.37)
EQE (%)(maximum)	16.6	21.0	18.9	18.6

Table 8. Key parameters from $Bebq_2$:$Ir(phq)_2acac$ (0.5 – 2 wt%) orange-red emitting ITO/DNTPD (40nm) / $Bebq_2$: $Ir(phq)_2acac$ (50 nm, 0.5 to 2%)/ LiF(0.5 nm) /Al(100 nm) PHOLED devices.

Indeed, because of the extraordinarily low doping concentration (~ 1%) by contrast with most phosphorescent devices (6 ~ 10 wt%), the enhancement of the performance of $Bebq_2$:$Ir(phq)_2acac$ PHOLEDs was never expected. In order to investigate the origin for the enhanced performance, we fabricated several PHOLEDs by varying the doping concentration from 0.5 to 2% in the host-guest system. Current and luminance as a function of voltage are presented in Fig. 19(a), while current and power efficiencies as a function of luminance are presented in Fig. 19(b). This data provides evidence for: (1) complete energy transfer from the fluorescent host to phosphorescent guest, except at extremely low doping concentrations (~0.5%); (2) no significant difference between measured I-V characteristics for identical devices but with different dopant concentrations lying between 0.5 and 2 wt%;

and, (3) the quenching of both luminance, and current and power efficiencies with higher doping concentrations (~ 2 wt%). A summary of the key electrical and optical parameters (Table 8) reveals the excellent device performance for doping concentration as low as 0.5 – 2%, in contrast with conventional PHOLEDs which require a guest concentration typically in the range of 6 to 10 wt%. Therefore, a highly efficient simple bilayer PHOLED structure with a $Ir(phq)_2acac$ guest doping concentration as low as 1% in the narrow band gap $Bebq_2$ fluorescent host is demonstrated here. Previously, $(ppy)_2Ir(acac):Ir(piq)_3$ (0.3 – 1wt %) red (Tsuzuki & Tokito, 2007) and CBP:$Ir(phq)_2acac$ (6 wt%) orange-red PHOLEDs (Kwong et al. 2002) demonstrated an EQE of 9.2% with a power efficiency of 11.0 lm/W and a power efficiency of 17.6 cd/A with an EQE of 10.3% at 600 nit, respectively.

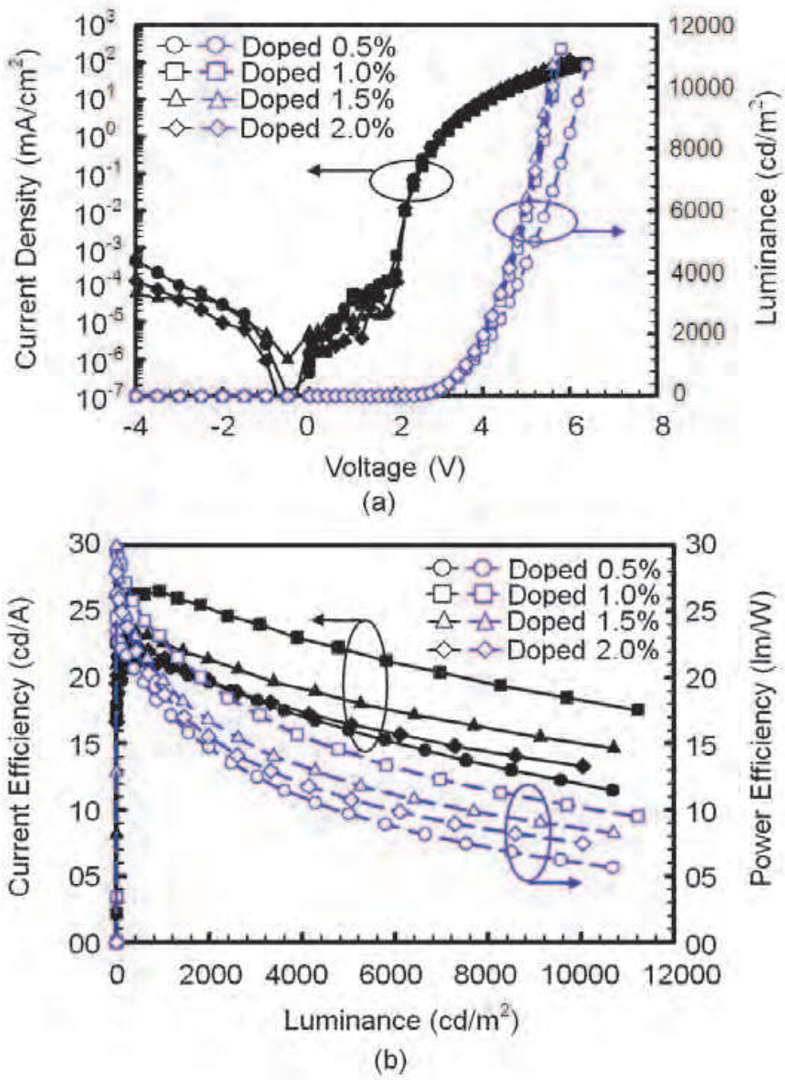

Fig. 19. (a) A J-V-L plot and (b) Current and power efficiencies as a function of luminance from red PHOLEDs doped with different concentrations (0.5 – 2 %) of $Ir(phq)_2acac$.

Figure 20 provides an evidence of energy transfer from the $Bebq_2$ fluorescent host to the $Ir(phq)_2acac$ phosphorescent guest by comparing the electroluminescence (EL) spectra of

PHOLEDs as a function of $Ir(phq)_2acac$ doping concentration from 0.5 to 2%. The strong red light emission peak at 605 nm for all EL curves at 1000 nit is attributed to the phosphorescence of $Ir(phq)_2acac$. The Commission Internationale de l'Eclairage (CIE) color emission coordinates are (0.61, 0.38), (0.62, 0.37), (0.62, 0.37), (0.62, 0.37) for doping concentrations of 0.5, 1.0, 1.5, and 2.0 wt% of $Ir(phq)_2acac$, respectively (as seen in Fig. 21). A slight emission at 500 nm due to the $Bebq_2$ host plus a dominant doping peak at 605 nm when the doping concentration is extremely low (~ 0.5%), suggests an incomplete energy transfer from the $Bebq_2$ host to the $Ir(phq)_2acac$ guest. Furthermore, it indicates that the recombination of injected holes and electrons occurs at host molecule sites and then the excited energy is rapidly transferred from the host to the guest. The presence of a clean EL peak (no emissions at 500 nm) in other devices with doping concentrations of $Ir(phq)_2acac$ > 0.5% indicates a complete energy transfer from the host to the guest.

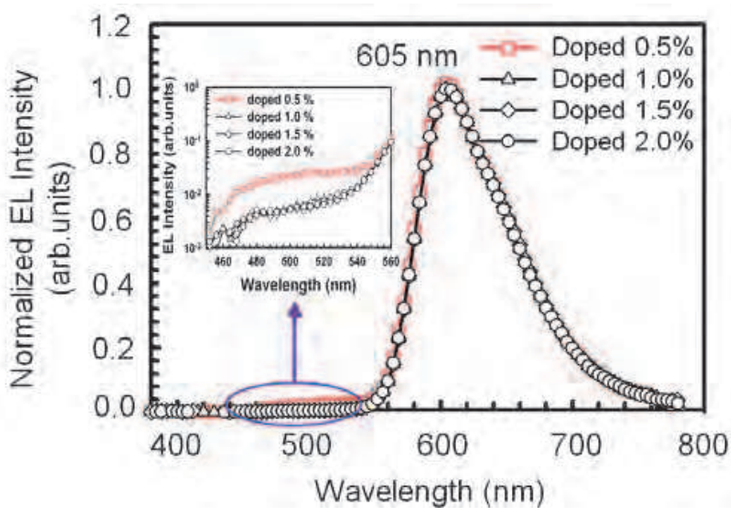

Fig. 20. EL spectra as a function of dopant concentration: $Ir(phq)_2acac$ of an ITO/DNTPD (40 nm) / $Bebq_2$: $Ir(phq)_2acac$ (50 nm, 0.5 to 2%)/ LiF(0.5 nm) / Al(100 nm) PHOLEDs at 1000 cd/m^2.

To understand the phosphorescence emission mechanism more precisely in the $Bebq_2$:$Ir(phq)_2acac$ host-guest system, we fabricated a series of PHOLEDs and studied. At first, we used the well known wide band gap CBP host material instead of $Bebq_2$ and fabricated the multilayer devices with a structure: NPB (40nm) / CBP:$Ir(piq)_3$ (30nm, 10%) / BAlq (5nm) / Alq_3 (20nm) / LiF (0.5nm) / Al (100nm) (Device A) and NPB (40nm) / CBP:$Ir(phq)_2acac$ (30nm, 10%) / BAlq (5nm) / Alq_3 (20nm) / LiF (0.5nm) / Al (100nm) (Device B). Table 9 displays the electrical performance of the fabricated phosphorescent devices. At a luminance of 1000 cd/m^2 the resultant operating voltage was 7.1 V with current and power efficiencies of 14.41 cd/A and 6.28 lm/W, respectively, and an EQE of 11.5%. Furthermore, the maximum current and power efficiency values were 14.43 cd/A and 8.99 lm/W, respectively. Obviously, the two fold increase in driving voltage is a consequence of the trapping of injected holes and electrons at deep $Ir(phq)_2acac$ molecules in the CBP:$Ir(phq)_2acac$ system. Direct charge trapping on the $Ir(phq)_2acac$ guest molecules seems to be the key mechanism for phosphorescence emission in this host-guest system.
Later, bilayer PHOLED device was fabricated using $Ir(piq)_3$ red emitting phosphorescent doping instead of $Ir(phq)_2acac$ and a $Bebq_2$ host. The fabricated devices were: DNTPD

(40nm) / $Bebq_2$:$Ir(piq)_3$ (50 nm, 4~10 wt%) / LiF (0.5 nm) / Al (100 nm). Current density-Voltage-Luminance and current and power efficiencies as a function of luminance plots are shown in Fig. 22. Electrical performances of the fabricated phosphorescent devices are illustrated in Table 10. A weak emission peak at 500 nm in the EL spectra due to the $Bebq_2$ host arises at a doping concentration of 4 wt% (significantly high by comparison with an $Ir(phq)_2acac$ doping concentration ~ 0.5 wt%), accompanied by a strong peak at 620 nm (CIE coordinates x = 0.67 and y = 0.32) due to an $Ir(piq)_3$ doping molecule (Fig. 23). At luminance of 1000 cd/m², the corresponding operating voltage, current and power efficiencies were 3.5V, 8.41 cd/A and 7.34 lm/W, respectively. Furthermore, the maximum current and power efficiency values were 9.38 cd/A and 11.72 lm/W, respectively. Increasing the $Ir(piq)_3$ concentration to 6 wt% suppresses the $Bebq_2$ host emission and results in a clean EL red emitting peak at 620 nm due to the $Ir(piq)_3$ doping molecules. However, the device performance deteriorates with increasing doping concentration due to a self quenching process as seen in Table 10.

Parameters	Device A CBP:$Ir(piq)_3$	Device B CBP:$Ir(phq)_2acac$
Turn-on voltage (at 1 cd/m²)	3.3 V	3.1 V
Operating voltage (1000 cd/m²)	7.2 V	7.1 V
Efficiency (1000 cd/m²)	5.71 cd/A 2.49 lm/W	14.41 cd/A 6.28 lm/W
Efficiency (Maximum)	6.47 cd/A 4.45 lm/W	14.43 cd/A 8.99 lm/W
CIE (x,y) (1000 cd/m²)	(0.66, 0.33)	(0.61, 0.38)
Quantum efficiency (maximum)	11.2 %	11.5 %
Roll off (1000 nt vs 10000 nt)	48 %	86 %

Table 9. Electrical performance of the multilayer CBP:$Ir(piq)_3$ (Device A) and CBP:$Ir(phq)_2acac$ (Device B) fabricated phosphorescent devices

The primary mechanism for the phosphorescence emission in the $Bebq_2$:$Ir(piq)_3$ host-guest system (Fig. 18 (b)) appears to be due to the energetically favorable electron transport and hole trapping at deep trapping centers in $Ir(piq)_3$ molecules. Thus, an appropriate selection of the host and phosphorescent dopant materials plays a significant role in determining the emission mechanism on phosphorescent devices. These results on phosphorescent emission in $Bebq_2$:$Ir(phq)_2acac$ host-guest systems are very interesting and intriguing. The mechanism of phosphorescence emission is not believed to be due to the direct charge trapping in $Ir(phq)_2acac$ phosphorescent guest molecules. Attempts have been made here to explain these results on the basis of the existing knowledge of Förster and Dexter energy transfer processes in host-guest systems.

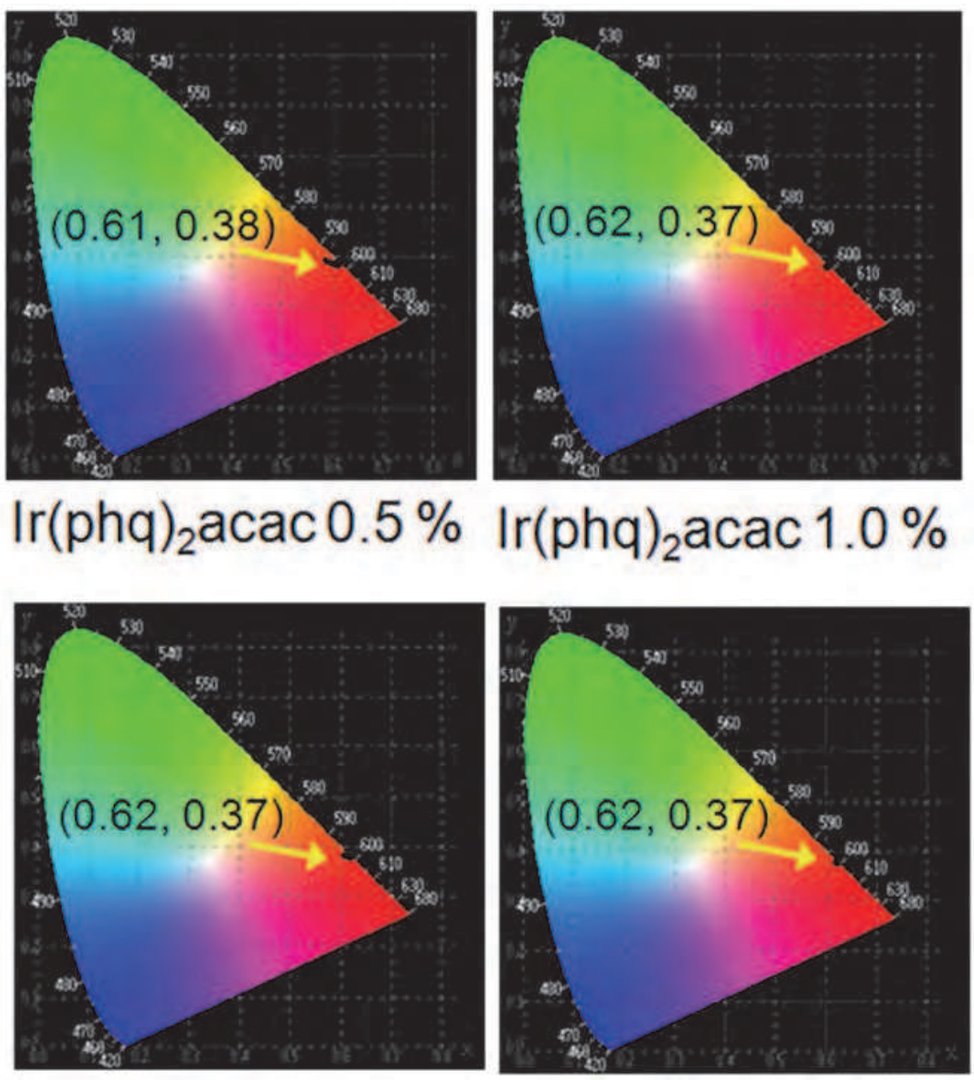

Fig. 21. Commission Internationale de l'Eclairage (CIE) color emission coordinates of red PHOLEDs described in Fig. 20.

The $Bebq_2$ host material produces a strong fluorescence emission but no phosphorescence emission signature even at 77 K. The efficient use of $Bebq_2$ host in the described phosphorescent devices is an extraordinary phenomenon since strong fluorescent host materials are believed to provide poor phosphorescent performance. Therefore, we suspect efficient Förster energy transfer between the host singlet and the metal-to-ligand charge-transfer (MLCT) state of the iridium (III) metal complex. Earlier, Förster energy transfer in phosphorescent OLEDs was postulated by Gong *et al.* and Ramos-Ortiz. *et al.* in solid photoluminescence studies (Gong et al., 2003; Ramos-Ortiz et al., 2002). To investigate Förster energy transfer from the $Bebq_2$ host to the $Ir(phq)_2acac$, time resolved spectroscopy and a Stern-Volmer plot in THF solution measurements techniques were employed. The

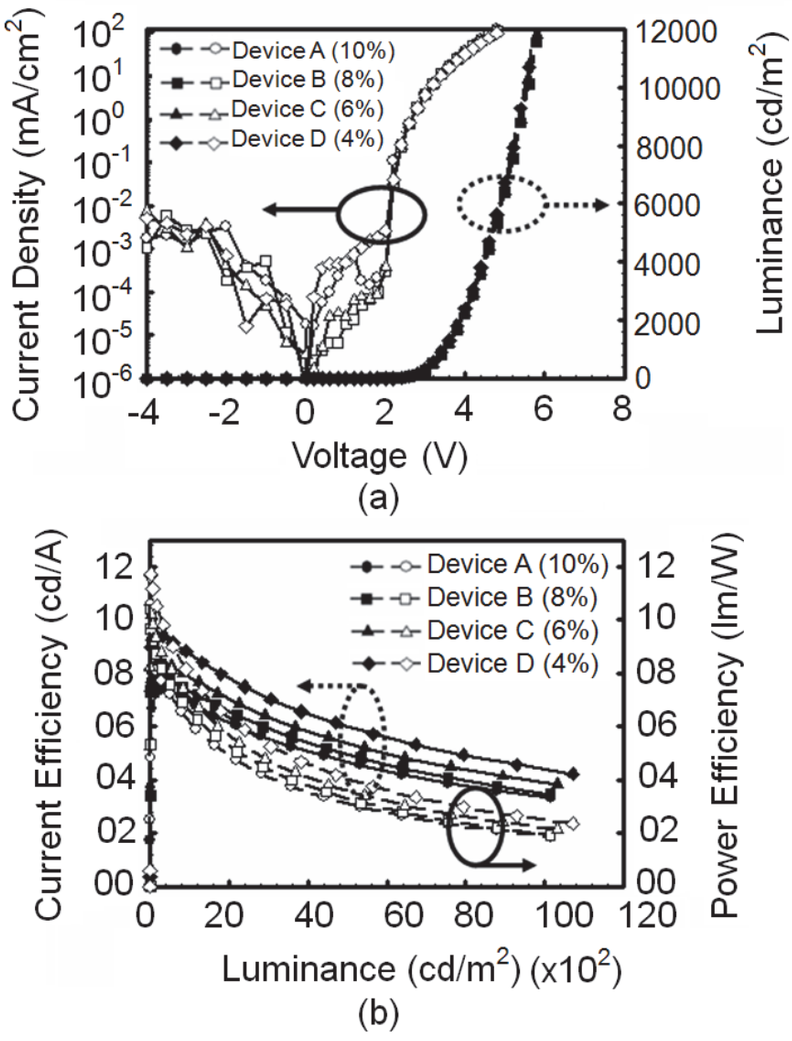

Fig. 22. Current density-Voltage-Luminance and current and power efficiencies as a function of luminance plots of DNTPD (40nm) / $Bebq_2$:$Ir(piq)_3$ (50 nm, 4~10 wt%) / LiF (0.5 nm) / Al (100 nm) red PHOLEDs

singlet fluorescent lifetime of $Bebq_2$ is 5.0 *ns*. From the slope of the linear Stern-Volmer plot (Fig. 24), the calculated energy transfer rate is $k_q = 8\times10^{12}$ $sec^{-1}M^{-1}$, indicating that the energy transfer from the excited singlet state of the host to the dopant triplet occurs quantitatively and ideally. Furthermore, the strong spin orbital coupling induced by the transition metal ion indicates that a narrow energy gap exists between the ^{1}MLCT and ^{3}MLCT states (~ 0.3eV) and opens a pathway for efficient energy transfer from the singlet to the emitting triplet states. Therefore, two channels for Förster energy transfer from the host singlet to the ^{1}MLCT and ^{3}MLCT states of the iridium complex are available as shown in Fig. 25. Overlapping of the host emission and dopant absorption spectra substantiates the hypothesis of efficient Förster energy transfer from the host singlet to the guest emitting triplet states via two channels (Fig. 26). Furthermore, the strong fluorescent quantum efficiency of 0.39 in the host ($Bebq_2$) in solution, obtained using a relative quantum yield measurement, favors Förster energy transfer.

Parameters	Device A (10%)	Device B (8%)	Device C (6%)	Device D (4%)
Turn-on voltage (at 1 cd/m²)	2.1 V	2.1 V	2.1 V	2.1 V
Operating voltage (1000 cd/m²)	3.5 V	3.5 V	3.5 V	3.5 V
Efficiency (1000 cd/m²)	6.78 cd/A 5.92 lm/W	7.18 cd/A 6.26 lm/W	7.65 cd/A 6.68 lm/W	8.41 cd/A 7.34 lm/W
Efficiency (Maximum)	7.38 cd/A 8.10 lm/W	7.82 cd/A 10.40 lm/W	8.37 cd/A 10.67 lm/W	9.38 cd/A 11.72 lm/W
CIE (x,y) (1000 cd/m²)	(0.67,0.32)	(0.67,0.32)	(0.67,0.32)	(0.67,0.32)
Quantum efficiency (maximum)	11.4 %	13.0 %	14.4 %	16.3 %
Roll off (1000 nt vs 10000 nt)	48 %	48 %	50 %	47 %

Table 10. Electrical performances of the fabricated DNTPD (40nm) / $Bebq_2$:$Ir(piq)_3$ (50 nm, 4~10 wt%) / LiF (0.5 nm) / Al (100 nm) red phosphorescent devices

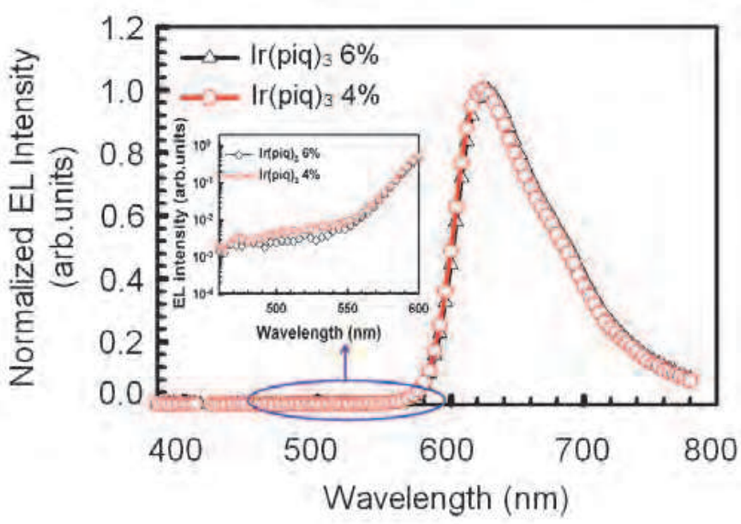

Fig. 23. EL spectra of DNTPD (40nm) / $Bebq_2$:$Ir(piq)_3$ (50 nm, 4 and 6 wt%) / LiF (0.5 nm) / Al (100 nm) PHOLEDs at 8000 cd/m².

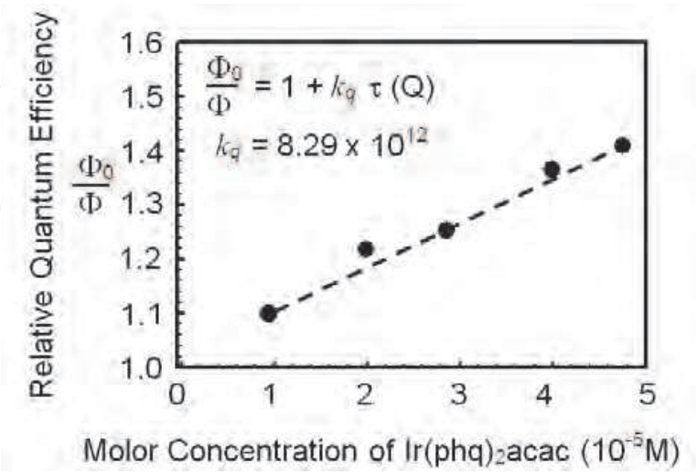

Fig. 24. Stern-Volmer plot showing the effect of $Bebq_2$ fluorescence quenching by ($Ir(phq)_2acac$) dopant.

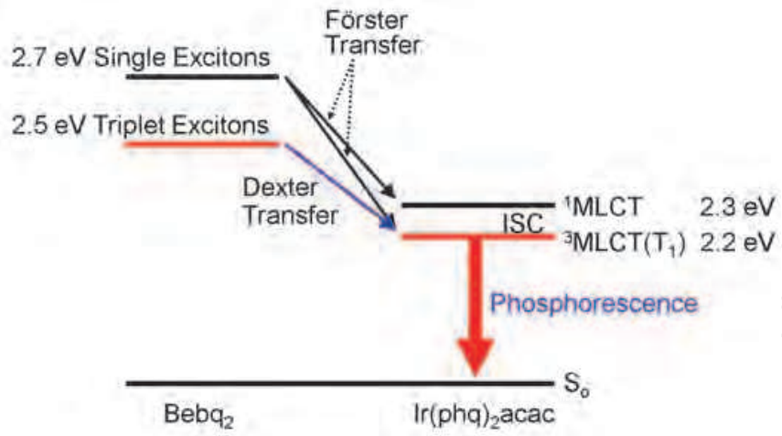

Fig. 25. Förster and Dexter energy transfer mechanism in the $Bebq_2$:$Ir(phq)_2acac$ system.

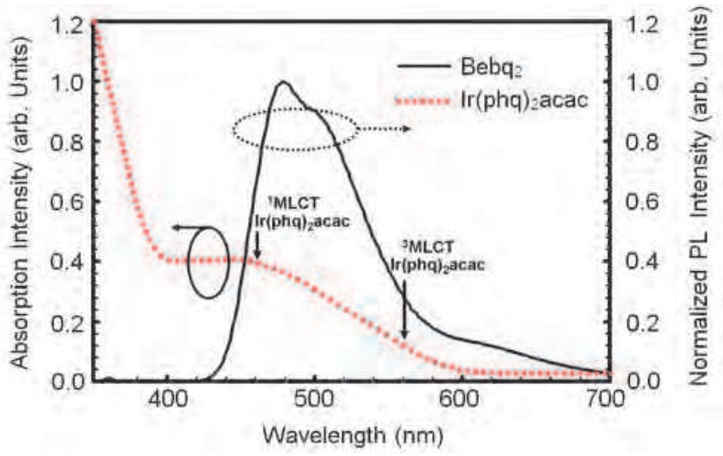

Fig. 26. Spectral overlapping of the photoluminescence spectrum from $Bebq_2$ and the absorption spectrum from $Ir(phq)_2acac$.

The Förster radius (R_0), critical distance for the concentration quenching, was estimated as 1.3 *nm* (similar to a previously reported value) using the following equation:

$$R_0^6 = \frac{9000(\ln 10)k^2\Phi_{PL}}{128\pi^5 N_A n^4}\int_0^\infty F_D(\lambda)\varepsilon_A(\lambda)\lambda^4 d\lambda$$

where k^2 = orientation factor, Φ_{PL} = photoluminescence quantum efficiency, N_A = Avogadro's number, n = refractive index, $\int_0^\infty F_D(\lambda)\varepsilon_A(\lambda)$ = spectral overlap integral between donor photoluminescence ($F_D(\lambda)$), and $\varepsilon_A(\lambda)$ = acceptor absorption, and λ = wavelength.

The triplet exciton energy transfer from the $Bebq_2$ host to ^{3}MLCT is governed by Dexter energy transfer. The rate constant of Dexter energy transfer (Kawamura et al., 2006) is

$$k_{ET} = K\,J \exp(-2R_{DA}/L)$$

where K is related to the specific orbital interaction, J is a spectral overlap integral, and R_{DA} is donor-acceptor separation relative to their van der Waals radii, L. The ideal Dexter radius is the distance between the host and dopant molecule diameter considering overlapping molecular orbitals in adjacent molecules (Turro, 1991a).

Using the equation: R = [(molecular density in film) × mol% of the dopant in a film]$^{-1/3}$ as reported by Kawamura et al. (Kawamura et al., 2006) yields an average distance of about 58.5Å and 44.9Å between $Ir(phq)_2acac$ molecules for doping concentrations of 0.5%, 1.0%, respectively (Fig.27). By considering the host (13.6Å) and dopant (13.7Å) diameters calculated using a molecular modeling program (DMOL3) (Delley, 2000) and van der Waals interaction distance (usually very small ~ within 2Å) for the ideal Dexter energy transfer condition, the estimated distance between the host and guest molecules is about 15.6Å (i.e. the half diameters of the host and dopant molecules are, 13.7/2Å plus 13.6Å/2, including a 2Å van der Waals interaction distance). In solid state films, the minimum doping concentration is desirable to prevent triplet quenching processes.

Considering that two host molecules are located between two dopant molecules, an ideal Dexter condition (Fig. 27(b)), all host molecules are adjacent to a dopant molecule and dopant molecules are well separated in the host matrix. In such a host and guest molecule arrangement, the separation between two dopant molecules appears to be about 46.9Å. However, when the doping concentration is 0.5%, the estimated separation between $Ir(phq)_2acac$ molecules is 58.5Å, suggesting that more than two host molecules are located between two dopant molecules (Fig. 27(b). If the doping concentration is increased to 1%, the separation between dopant molecules is less than 46.9Å, which results in an efficient energy transfer from the $Bebq_2$ host to the emitting triplet state of $Ir(phq)_2acac$ via Dexter processes. The triplets generated due to the $Bebq_2$ host molecules diffuse to an average distance of only 15.6Å, with a doping concentration of 1 wt%, until they are harvested by $Ir(phq)_2acac$ (Fig. 27(b). If the doping concentration is increased to greater than 1%, the device performance deteriorates due to quenching processes of triplet excitons caused by two closely separated dopant molecules.

The influence of the Förster quenching process in the described system is not serious at all doping concentrations (Fig. 27(a). The singlet exciton energies generated by charge injection in host molecules can be transferred to triplet states of dopant molecules by the efficient Förster energy transfer. In our system, the rate constant of Förster energy transfer is much faster than that of the intersystem crossing of host singlet states. Typical intersystem crossing rate constants fall within the range ~10^6-10^8 sec^{-1} (Turro, 1991b). Thus, strong fluorescent materials, such as $Bebq_2$, are excellent as host materials in PHOLEDs.

6.4 Conclusions

In conclusion, we have demonstrated here an ideal host-guest energy transfer and quantum efficiency conditions with a dopant concentration of approximately 1% in phosphorescent OLEDs. We also report that strong fluorescent host materials function very well in phosphorescent OLEDs. The operating mechanism for the phosphorescence emission is twofold: Firstly, an efficient Förster energy transfer process from the host singlet exciton to the ^{1}MLCT and ^{3}MLCT states of the guest. And, secondly, a Dexter energy transfer process from the host triplet exciton to the ^{3}MLCT state of the guest. The extremely low doping concept for highly efficient PHOLEDs has potential uses in future display and lighting applications.

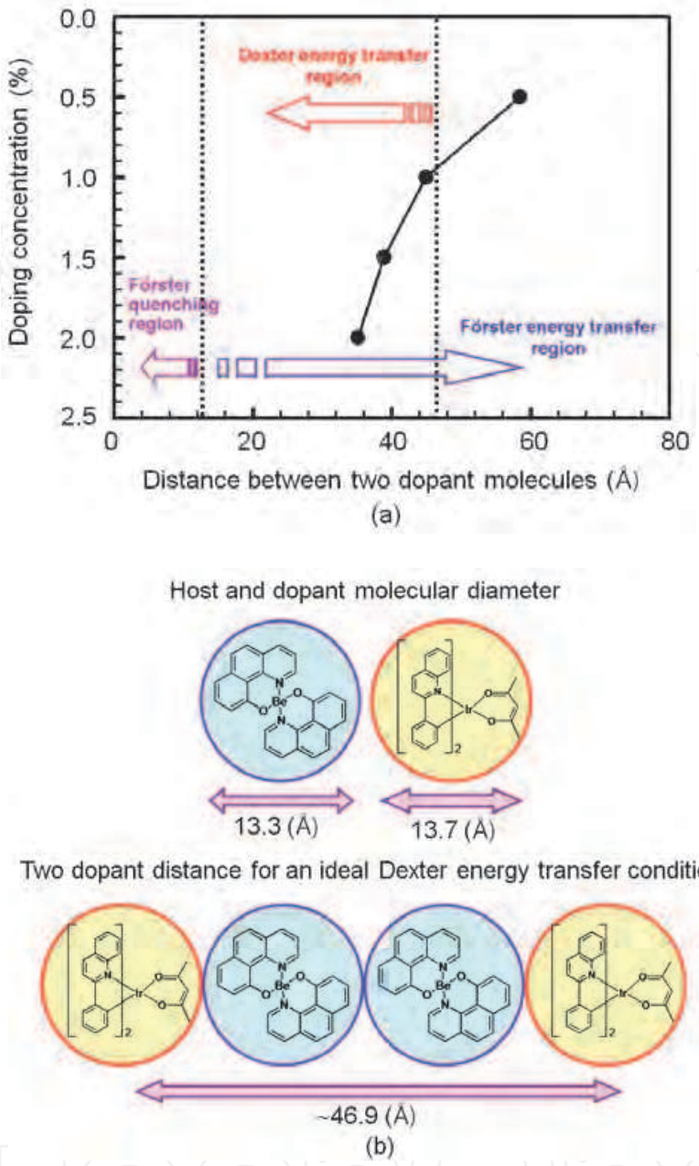

Fig. 27. (a) Förster and Dexter energy transfer conditions as a function of doping concentration and distance between two dopants. (b) The molecular diameters of the host and dopant and the dopant-dopant distance for an ideal Dexter energy transfer.

7. Conclusions

Simple structure red PHOLED, using **narrow band gap fluorescent host materials have been demonstrated**, having a:

(1) Simple structure, (2) Low driving voltage, (3) High efficiency (lm/W), (4) No charge trapping at phosphorescent guest molecules, (5) Low doping concentration, and (6) Low manufacturing cost.

These results are summarized in Table 11. Various triplet quantum well devices from a single to five quantum wells are realized using a wide band-gap hole and an electron transporting layers, $Bebq_2$ narrow band-gap host and $Ir(piq)_3$ red dopant materials, and

$Bepp_2$ charge control layers (CCL). Triplet energies in fabricated MQW devices are confined at the emitting layers. The maximum external quantum efficiency of 14.8 % with a two quantum well device structure is obtained, which is the highest value among the reported $Ir(piq)_3$ dopant red phosphorescent OLEDs. The described MQW device concept can be very useful to future OLED display and lighting applications.

Parameters	[1]MQW p-i-n device n=2	[2]Bilayer device	[3]Single Layer 4% Doping	[4]Single Layer 1% Doping	[5]Ideal host-Guest Device (1%)
Turn on voltage (@ 1cd/m²)	2.5 V		2.3 V	2.4 V	2.1
Operating voltage (@ 1000 cd/m²)	4.2 V	4.5V	6.9 V	5.4 V	3.7
Current (cd/A) & Power (lm/W) efficiencies @ 1000 cd/m²		9.66, 6.90	7.44, 3.43	9.02, 5.25	20.53 23.14
Maximum Current (cd/A) & Power (lm/W) Efficiencies	12.4		8.04, 10.96	9.44, 10.62	26.53, 29.58
CIE (x, y) (@ 1000 cd/m²)	(0.66, 0.33)	(0.67, 0.33)	(0.67, 0.32)	(0.66, 0.33)	(0.62, 0.37)
EQE (%) (maximum)	14.8				21.0

[1]ITO/TCTA:WO_3(30%,40nm)/TCTA(12nm)/**$Bebq_2$:Ir(2%,10nm)/$Bepp_2$(CCL,5nm)(n=2)** /$Bepp_2$ (7 nm)/$Bepp_2$:Cs_2CO_3 (10%, 20 nm)/ Al(100 nm)
[2]ITO/α-NPB (40 nm) / **$Bebq_2$: $Ir(piq)_3$ (10 wt%, 50 nm)**/ LiF(0.5 nm) / Al(100 nm
[3]ITO/**m-MTDATA:$Bebq_2$: $Ir(piq)_3$ (4 wt%, 100 nm)**/LiF (0.5 nm)/Al (100 nm)
[4]ITO/**α-NPB:$Bebq_2$: $Ir(piq)_3$ (1 wt%, 100 nm)**/LiF (0.5 nm)/Al (100 nm).
[5]ITO/DNTPD (40nm) / **$Bebq_2$: $Ir(phq)_2acac$ (50 nm, 1%)**/ LiF(0.5 nm) /Al(100 nm)

Table 11. Summary of performances of red PHOLEDs in this study

Bi-layered simple structure red PHOLED demonstrates high current and power efficiency values of 9.66 cd/A and 6.90 lm/W, respectively. The operating voltage of bi-layered PHOLEDs at a luminance of 1000 cd/m² was 4.5 V. A simple bilayerd red emitting device with $Bebq_2$ host could be a promising way to achieve efficient, economical, and ease manufacturing process, important for display and lighting production.

We have also demonstrated high efficiency red PHOLEDs comprising only single emitting layer. The driving voltage of 5.4 V to reach the 1000 cd/m² and maximum current and power efficiency values of 9.44 cd/A and 10.62 lm/W, respectively, in the α-NPB/ $Bebq_2$ mixed single layer structure PHOLEDs with the $Ir(piq)_3$ dopant as low as 1 wt% are obtained. The obtained results could be useful to simplify the device structure with a reasonable reduction in the manufacturing cost of passive and active matrix OLEDs.

An ideal host-guest system displays efficient energy transfer and quantum efficiency conditions with a dopant concentration of approximately 1% in phosphorescent OLEDs. A luminance of 1000 cd/m² was obtained with a driving voltage of 3.7 V, and current and power efficiencies of 20.53 cd/A and 23.14 lm/W (maximum current efficiency: 26.53 cd/A and maximum power efficiency: 29.58 lm/W), respectively. The external quantum efficiency (EQE) value of 21% in the fabricated PHOLED, slightly exceeded the theoretical limit of about 20% derived from simple classical optics, is recorded.

In summary, narrow band gap fluorescent host materials with the extremely low doping concept for highly efficient PHOLEDs has potential uses in future display and lighting applications.

8. Acknowledgement

Authors are thankful to Professor Yup Kim, Physics Department (Kyung Hee University, Seoul) for his encouragement during the span of this work.

9. References

Al Attar, H.A., Monkman, A.P., Tavasli, M., Bettington, S. & Bryce, M.R. (2005). White polymeric light-emitting diode based on a fluorine polymer/Ir complex blend system, *Appl. Phys. Lett.* 86: 121101-1 – 121101-3.

Adachi, C., Baldo, M.A., Forrest, S.R. & Thompson, M.E. (2000). High-efficiency organic electrophosphorescent devices with tris(2-phenylpyridine)iridium doped into electron-transporting materials, *App. Phys. Lett.* 77: 904-906.

Adachi, C., Baldo, M.A., Forrest, S.R., Lamansky, S., Thompson, M.E. & Kwong, R.C. (2001a). High-efficiency red electrophosphorescence devices, *Appl. Phys. Lett*. 78: 1622-1624.

Adachi, C., Baldo, M. A., Thompson, M. E. & Forrest, S. R. (2001b). Nearly 100% internal phosphorescence efficiency in an organic light-emitting device, *J. Appl. Phys.* 90: 5048-5051.

Adamovich, V.I., Cordero, S.R., Djurovich, P.I., Tamayo, A., Thompson, M.E., D'Andrade, B. W. & Forrest, S.R. (2003). New charge-carrier blocking materials for high efficiency OLEDs, *Org. Electron*. 4 (2-3): 77-87.

Baldo, M.A., O'Brien, D.F., You, Y., Shoustikov, A., Sibley, S., Thompson, M.E. & Forrest, S.R. (1998). Highly efficient phosphorescent emission from organic electroluminescent devices, *Nature (London)* 395: 151-154.

Baldo, M. A., Lamansky, S., Burrows, P. E., Thompson, M. E. & Forrest, S. R. (1999). Very high-efficiency green organic light-emitting devices based on electrophosphorescence, *Appl. Phys. Lett.* 75: 4-6.

Baldo, M. A. & Forrest, S. R. (2000). Transient analysis of organic electrophosphorescence: I Transient analysis of triplet energy transfer, *Phy. Rev. B* 62, 10958-10966.

Bulovic, V., Khalfin, V. B., Gu, G. & Burrows, P. E. (1998). Weak microcavity effects in organic light-emitting devices, *Phys. Rev. B* 58: 3730-3740.

Che, G., Su, Z., Li, W., Chu, B., Li, M., Hu, Z. & Zhang, Z. (2006). Highly efficient and color-tuning electrophosphorescent devices based on Cu^{I} complex, *Appl. Phys. Lett.* 89: 103511-1 – 103511-3.

Chen, P., Xue, Q., Xie, W., Duan, Y., Xie, G., Hou, J., Liu, S., Zhang, L. & Li, B. (2008). Color-stable and efficient stacked white organic light-emitting devices comprising blue fluorescent and orange phosphorescent emissive units, *Appl. Phys. Lett*. 93: 153508-1 – 153508-3.

Chin, B. D., Suh, M. C., Kim, M. H., Lee, S. T., Kim, H. D. & Chung, H. K. (2005). Carrier trapping and efficient recombination of electrophosphorescent device with stepwise doping profile, *Appl. Phys. Lett.* 86: 133505-1 – 133505-3.

Coushi, K., Kwon, R., Brown, J. J., Sasabe, H. & Adachi, C. (2004). Triplet exciton confinement and unconfinement by adjacent hole-transport layers, *J. Appl. Phys.* 95: 7798-7802.

D'Andrade, B.W., Holmes, R.J. & Forrest, S.R. (2004). Efficient organic electrophosphorescent white-light-emitting device with a triple doped emissive layer, *Adv. Mater*. 16: 624-628.

D'Andrade, B. W. & Forrest, S. R. (2004). White organic light-emitting devices for solid- state lighting, *Adv. Mater.* (Weinheim, Ger.) 16: 1585-1595.

Delley, B. (2000). From molecules to solids with the DMoL3 approach, *J. Chem. Phys.* 113: 7756-7764.

Deng, Z. B., Ding, X. M., Lee, S.T. & Gambling, W.A. (1999). Enhanced brightness and efficiency in organic electroluminescent devices using SiO_2 buffer layers, *Appl. Phys. Lett.* 74: 2227-2279.

Destruel, P., Jolinat, P., Clergereaux, R. & Farenc, J. (1999). Pressure dependence of electrical and optical characteristics of Alq_3 based organic electroluminescent diodes, *J. Appl. Phys.* 85: 397-400.

Dexter, D.L. (1953). A Theory of Sensitized Luminescence in Solids, *J. Chem. Phys.* 21: 836-850.

Duan, J.-P., Sun, P.-P. & Cheng, C.-H. (2003). New iridium complexes as highly efficient orange-red emitters in organic light-emitting diodes, *Adv. Mater.* 15, 224-228.

Endo, J., Matsumoto, T. & Kido, J. (2002). Organic Electroluminescent Devices Having Metal Complexes as Cathode Interface Layer, *Jpn. J. Appl. Phys.* 41: L800-L803.

Forster, T. (1959). Transfer mechanisms of electronic excitation, *Discuss. Faraday Soc.* 27: 7-17.

Friend, R. H., Gymer, R. W., Holmes, A. B., Burroughes, J. H., Marks, R. N., Taliani, C., Bradley, D. D. C., Dos Santos, D. A., Bredas, J. L., Logdlund, M. & Salaneck, W. R. (1999). Electroluminescence in conjugated polymers, *Nature (London)* 397, 121-128.

Fukase, A. & Kido, J. (2002). High efficiency organic electroluminescent devices using Iridium complex emitter and arylamine-containing polymer buffer layer, *Polym. Adv. Technol*. 13: 601-604.

Gao, Y., Wang, L., Zhang, D., Duan, L., Dong, G. & Qiu, Y. (2003). Bright single-active layer small-molecular organic light-emitting diodes with a polytetrafluoroethylene barrier, *Appl. Phys. Lett.* 82: 155-157.

Giebeler, C., Antoniadis, H., Bradley, D. D. C. & Shirota, Y. (1998). Space-charge-limited charge injection from indium tin oxide into a starburst amine and its implications for organic light-emitting diodes, *Appl. Phys. Lett.* 72: 2448-2450.

Gong, X., Ostrowski, J.C., Moses, D., Bazan, G.C. & Heeger, A.J. (2002). Red electrophosphorescence from polymer doped with iridium complex, *App. Phys. Lett.* 81: 3711-3713.

Gong, X., Ostrowski, J.C., Moses, D., Bazan, G.C. & Heeger, A.J. (2003). Electrophosphorescence from a polymer guest-host system with an Iridium complex as guest: Forster energy transfer and charge trapping, *Adv. Funct. Mater.* 13: 439-444.

Hamada, Y., Sano, T., Fujita, M., Fujii, T., Nishio, Y. & Shibata, K. (1993). High luminance in organic electroluminescent devices with bis (10-hydroxybenzo [h]quinolinato) beryllium as an emitter, *Chem. Lett.* 22: 905-909.

Helfrich, W. & Schneider, W.G. (1965). Recombination Radiation in Anthracene Crystals, *Phys. Rev. Lett.* 14: 229-231.

Ho, C.-L., Wong, W.-Y., Wang, Q., Ma, D., Wang, L. & Lin, Z. (2008a). A Multifunctional Iridium-Carbazolyl Orange Phosphor for High-Performance Two-Element WOLED Exploiting Exciton-Managed Fluorescence/Phosphorescence, *Adv. Funct. Mater*. 18: 928-937.

Ho, C.-L., Lin, M.-F., Wong, W.-Y., Wong, W.K. & Chen, C.H. (2008b). High-efficiency and color-stable white organic light-emitting devices based on sky blue electrofluorescence and orange electrophosphorescence, *Appl. Phys. Lett.* 92: 083301-1 – 083301-3.

Holmes, R.J., D'Andrande, B.W., Ren, X., Li, J., Thompson, M.E. & Forrest, S.R. (2003). Efficient, deep-blue organic electrophosphorescence by guest charge trapping, *Appl. Phys. Lett.* 83: 3818-3820.

Hong, I-H., Lee, M.-W., Koo, Y.-M., Jeong, H., Kim, T.-S. & Song, O.-K. (2005). Effective hole injection of organic light-emitting diodes by introducing buckminsterfullerene on the indium tin oxide anode, *Appl. Phys. Lett.* 87: 063502-1 – 063502-3.

Huang, J., Yang, K., Liu, S. & Jiang, H. (2000). High-brightness organic double-quantum-well electroluminescent devices, *Appl. Phys. Lett.* 77: 1750-1752.

Huang, J., Pfeiffer, M., Werner, A., Blochwitz, J., Leo, K. & Liu, S. (2002). Low-voltage organic electroluminescent devices using *pin* structures, Appl. Phys. Lett. 80, 139-141.

Huang, Q., Cui, J., Yan, H., Veinot, J. G. C. & Marks, T. J. (2002). Small molecule organic light-emitting diodes can exhibit high performance without conventional hole transport layers, *Appl. Phys. Lett.* 81: 3528-3530.

Huang, J., Watanabe, T., Ueno, K. & Yang, Y. (2007). Highly Efficient Red Emission Polymer Phosphorescent Lighting Emitting Diodes based on two novel Ir(piq)3 derivatives, *Adv. Mater.* 19: 739-743.

Hung, L.S., Tang, C.W. & Mason, M.G. (1997). Enhanced electron injection in organic electroluminescence devices using an Al/LiF electrode, *Appl. Phys. Lett*. 70: 151-153.

Ikai, M., Tokito, S., Sakamoto, Y., Suzuki, T. & Taga, Y. (2001). Highly efficient phosphorescence from organic light-emitting devices with an exciton-block layer, *Appl. Phys. Lett.* 79: 156-158.

Jeon, W. S., Park, T. J., Park, J. J., Kim, S. Y., Jang, J., Kwon, J. H. & Pode, R. (2008a). Highly efficient bilayer green phosphorescent organic light emitting devices, *Appl. Phys. Lett*. 92: 113311-1 113311-3.

Jeon, W. S., Park, T. J., Park, J. J., Kim, S. Y., Pode, R., Jang, J. & Kwon, J. H. (2008b). Low roll-off efficiency green phosphorescent organic light-emitting devices with simple double emissive layer structure, *Appl. Phys. Lett*. 93: 063303-1 - 063303-3.

Jeon, W.S., Park, T. J., Kim, S. Y., Pode, R., Jang, J. & Kwon, J.-H. (2009). Ideal host and guest system in phosphorescent OLEDs *Org. Electron.* 10: 240-246.

Kawamura, Y., Goushi, K., Brooks, J., Brown, J., Sasabe, H. & Adachi, C. (2005). 100% phosphorescence quantum efficiency of Ir(III) complexes in organic semiconductor films, *Appl. Phys. Lett.* 86: 071104-1 – 071104-3.

Kawamura, Y., Brooks, J., Brown, J., Sasabe, H. & Adachi, C., (2006). Intermolecular Interaction and a Concentration-Quenching Mechanism of Phosphorescent Ir(III) Complexes in a Solid Film, *Phy. Rev. Lett.* 96: 017404-1 – 017404-4.

Kido, J. & Lizumi, Y. (1998). Fabrication of highly efficient organic electroluminescent devices, *Appl. Phys. Lett.* 73: 2721-2723.

Kim, H.-K., Byun, Y.-H., Das, R. R., Choi, B.-K. & Ahn, P.-S. (2007). Small molecule based and solution processed highly efficient red electrophosphorescent organic light emitting devices, *Appl. Phys. Lett.* 91: 093512-1 – 093512-3.

Kim, J. H., Liu, M. S., Jen, A. K. Y., Carlson, B., Dalton, L. R., Shu, C. F. & Dodda, R. (2003). Bright red-emitting electrophosphorescent device using osmium complex as a triplet emitter, *Appl. Phys. Lett.* 83: 776-778.

Kim, K.-K., Lee, J.-Y., Park, T.-J., Jeon, W.-S., Kennedy, G.P. & Kwon, J.-H. (2010). Small molecule host system for solution-processed red phosphorescent OLEDs, *Synthetic Met*. 160: 631-635.

Kim, S. H., Jang, J. S., Hong, J. M. & Lee, J. Y. (2007). High efficiency phosphorescent organic light emitting diodes using triplet quantum well structure, *Appl. Phys. Lett.* 90: 173501-1 – 173501-3.

Kim, S. Y., Jeon, W. S., Park, T. J., Pode, R., Jang, J. & Kwon, J. H. (2009). Low voltage efficient simple *p-i-n* type electrophosphorescent green organic light-emitting devices, *Appl. Phys. Lett.* 94: 133303-1 – 133303-3.

Kim, T.-H., Lee, H. K., Park, O. O., Chin, B. D., Lee, S.-H. & Kim, J. K. (2006). White-Light-Emitting Diodes Based on Iridium Complexes via Efficient Energy Transfer from a Conjugated Polymer, *Adv. Fun. Mater.* 16: 611-617.

Koo, Y.-M., Choi, S.-J., Chu, T.-Y., Song, O.-K., Shin, W.-J., Lee, J.-Y., Kim, J. C. & Yoon, T.-H. (2008). Ohmic contact probed by dark injection space-charge-limited current measurements, *J. Appl. Phys*. 104: 123707-1 – 123797-4.

Kwong, R.C., Nugent, M.R., Michalski, L., Ngo, T., Rajan, K., Tung, Y.-J., Weaver, M.S., Zhou, T.X., Hack, M., Thompson, M.E., Forrest, S.R. & Brown, J.J. (2002). High operational stability of electrophosphorescent devices, *Appl. Phys. Lett.* 81: 162-164.

Lamansky, S., Djurovich, P., Murphy, D., Abdel-Razzaq, F., Lee, H.-E., Adachi, C. Burrows, P.E., Mui, B., Forrest, S.R. & Thompson, M.E. (2001). Highly Phosphorescent Bis-Cyclometalated Iridium Complexes: Synthesis, Photophysical Characterization, and Use in Organic Light Emitting Diodes, *J. Am. Chem. Soc*. 40: 4304-4312.

Lee, T.-C., Chang, C.-F., Chiu, Y.-C., Chi, Y., Chan, T.-Y., Cheng, Y.-M., Lai, C.-H., Chou, P.-T., Lee, G.-H., Chien, C.-H., Shu, C.-F. & Leonhardt, J. (2009). Syntheses, photophysics, and application of iridium(III) phosphorescent emitters for highly efficient, long-life organic light-emitting diodes, *Chemistry – An Asian Journal* 4: 742-753.

Lee, J.-H., Lin, T.-C., Liao, C.-C. & Yang, F. H. (2005). Study on organic light-emitting device with more balanced charge transport, *Proc. of SPIE* 5632: 220-225.

Li, F., Cheng, G., Zhao, Y., Feng, F. & Liu, S.Y. (2003). White-electrophosphorescence devices based on rhenium complexes, *Appl. Phys. Lett.* 83: 4716-4719.

Liu, J., Zhou, Q., Cheng, Y., Geng, Y., Wang, L., Ma, D., Jing, X. & Wang, F. (2006). White electrolumineseence from a single-polymer system with simultaneous two-color emission, Polyfluorene as the blue host and a 2,1,3-benzothiadiazole derivative as the orange dopant on the main chain, *Adv. Funct.Mater.* 16: 957-965.

Liu, S. W., Huang, C. A., Lee, J. H., Yang, K. H., Chen, C. C. & Chang, Y. (2004). Blue mixed host organic light emitting devices, *Thin Solid Films* 453-454: 312-315.

Liu, Y., Guo, J., Feng, J., Zhang, H., Li, Y. & Wang, Y. (2001). High-performance blue electroluminescent devices based on hydroxyphenyl-pyridine beryllium complex, *Appl. Phys. Lett.* 78: 2300-2302.

Liu, Z. W., Helander, M. G., Wang, Z. B. & Lu, Z. H. (2009). Efficient bilayer phosphorescent organic light-emitting diodes: Direct hole injection into triplet dopants, *Appl. Phys. Lett.* 94, 113305-1 – 113305-3.

Liu, Z., Helander, M. G., Wang, Z. & Lu, Z. (2009). Efficient single layer RGB phosphorescent organic light-emitting diodes, *Organic Electron*.10: 1146-1151.

Liu, S. W., Lee, J. H., Lee, C. C., Chen, C. T. & Wang, J. K. (2007). Charge carrier mobility of mixed-layer organic light-emitting diodes, *Appl. Phys. Lett.* 91: 142106-1 – 142106-3.

Meyer, J., Hamwi, S., Bülow, T., Johannes, H.-H., Riedl, T. & Kowalsky, W. (2007). Highly efficient simplified organic light emitting diodes, *Appl. Phys. Lett.* 91: 113506-1 – 113506-3.

Mi, B. X., Wang, P. F., Gao, Z. Q., Lee, C. S., Lee, S. T., Hong, H. L., Chen, X. M., Wong, M. S., Xia, P. F., Cheah, K. W., Chen, C. H. & Huang, W. (2009). Strong Luminescent Iridium Complexes with C^N=N Structure in Ligands and Their Potential in Efficient and Thermal-stable Phosphorescent OLEDs, *Adv. Mater.* 21: 339-343.

Ohmori, Y., Kajii, H. & Hino, Y. (2007). Organic Light-Emitting Diodes Fabricated by a Solution Process and Their Stress Tolerance, *J. of Display Technology* 3: 238-244.

Park, T.-J., Jeon, W.-S., Park, J.-J., Kim, S.-Y., Lee, Y.-K., Jang, J., Kwon, J.-H. & Pode, R. (2008). Efficient simple structure red phosphorescent organic light emitting devices with narrow band-gap fluorescent host, *Appl. Phys. Lett.* 92: 113308-1 – 113308-3.

Pfeiffer, M., Forrest, S.R., Leo, K. & Thompson, M.E. (2002). Electrophosphorescent p-i-n organic light-emitting devices for very-high- efficiency flat-panel displays, *Adv. Mater.* 14: 1633-1636.

Pode, R., Kim, K.-H., Kwon, J.-H., Lee, S.-J., Shin, I.-A. & Jin, S.-H. (2010). Solution processed efficient orange phosphorescent organic light-emitting device with small molecule host, *J Phys. D: Appl. Phys.* 43: 025101-1 – 025101-5.

Pode, R., Ahn, J.-S., Jeon, W. S., Park, T. J. & Kwon, J.-H. (2009). Efficient red light phosphorescence emission in simple bi-layered structure organic devices with fluorescent host-phosphorescent guest system, *Current Applied Physics* 9, 1151-1154.

Pope, M., Kallmann, H.P. & Magnante, P. (1963). Electroluminescence in Organic Crystals, *The Journal of Chemical Physics* 38: 2042- 2043.

Qiu, Y., Gao, Y., Wei, P. & Wang, L. (2002a). Organic light-emitting diodes with improved hole-electron balance by using copper phthalocyanine/aromatic diamine multiple quantum wells, *Appl. Phys. Lett.* 80: 2628-2630.

Qiu, Y., Gao, Y., Wang, L., Wei, P., Duan, L., Zhang, D. & Dong, G. (2002b). High-efficiency organic light-emitting diodes with tunable light emission by using aromatic diamine/5,6,11,12-tetraphenylnaphthacene multiple quantum wells, *Appl. Phys. Lett.* 81: 3540-3542.

Ramos-Ortiz, G., Oki, Y., Domercq, B. & Kippelen, B. (2002). Förster energy transfer from a fluorescent dye to a phosphorescent dopant: a concentration and intensity study, *Physical Chemistry Chemical Physics (RSC Publishing)* 4: 4109-4114.

Sheats, J. R., Antoniadis, H., Hueschen, M., Leonard, W., Miller, J., Moon, R., Roitman, D. & Stocking, A. (1996). Organic Electroluminescent Devices, *Science* 273: 884-888.

Shirota, Y., Kuwabara, Y., Inada, H., Wakimoto, T. , Nakada, H., Yonemoto, Y., Kawami, S. & Imai, K. (1994). Multilayered organic electroluminescent device using a novel starburst molecule, 4,4',4"-tris(3-methylphenylphenylamino)triphenylamine, as a hole transport material, *Appl. Phys. Lett*. 65: 807-809.

Seo, J.H., Park, J.H., Kim, Y.K., Kim, J.H., Hyung, G.W., Lee, K.H. & Yoon, S.S. (2007). Highly efficient white organic light-emitting diodes using two emitting materials for three primary colors (red, green, and blue), *Appl. Phys. Lett.* 90: 203507-1 – 203507-3.

Shen, Z., Burrows, P. E., Bulovic, V., Forrest, S. R. & Thompson, M. E. (1997). Three-Color, Tunable, Organic Light-Emitting Devices, *Science* 276: 2009-2011.

Shoustikov, A., You, Y., Burrows, P.E., Thompson, M.E. & Forrest, S.R. (1997). Orange and red organic light-emitting devices using aluminum tris(5-hydroxyquinoxaline), *Synth. Met.* 91, 217-221.

Tanaka, D., Sasabe, H., Li, Y.J., Su, S.-J., Takeda, T. & Kido, J. (2007). Ultra High Efficiency Green Organic Light-Emitting Devices, *Jpn. J. Appl. Phys. 2 Lett. (Japan)* 46: L10-L12.

Tanaka, I. & Tokito, S. (2008). Energy-transfer processes between phosphorescent guest and fluorescent host molecules in phosphorescent OLEDs, Edited by H. Yersin, *Highly efficient OLEDs with Phosphorescent materials*, Wiley –VCH verlag GmbH & Co. KGaA, Weinheim.

Tanaka, I., Tabata, Y. & Tokito, S. (2004). Energy-transfer and light-emission mechanism of blue phosphorescent molecules in guest-host systems, *Chem. Phys. Lett*. 400: 86-89.

Tang, C.W., Chen, C. H. & Goswami, R. (1988). Electroluminescent device with modified thin film luminescent zone, US Patent No. 4 769 292.

Tse, S. C., Tsung, K. K. & So, S. K. (2007). Single-layer organic light-emitting diodes using naphthyl diamine, *Appl. Phys. Lett.* 90: 213502-1 – 213502-3.

Tse, S. C., Tsang, S. W. & So, S. K. (2006). Polymeric conducting anode for small organic transporting molecules in dark injection experiments, *J. Appl. Phys.* 100: 063708-1 – 063708-5.

Tsuboi, T., Jeon, W. S. & Kwon, J. H. (2009). Observation of phosphorescence from fluorescent organic material $Bebq_2$ using phosphorescent sensitizer, *Opt. Mater.* 31: 1755-1758.

Tsuboyama, A., Iwawaki, H., Furugori, M., Mukaide, T., Kamatani, J., Igawa, S., Moriyama, T., Miura, S., Takiguchi, T., Okada, S., Hoshino, M. & Ueno, K. (2003). Homoleptic Cyclometalated Iridium Complexes with Highly Efficient Red Phosphorescence and Application to Organic Light-Emitting Diode, *J. Am. Chem. Soc.* 125: 12971-12979.

Tsujimoto, H., Yagi, S., Asuka, H., Inui, Y., Ikawa, S., Maeda, T., Nakazumi, H. & Sakurai, Y. (2010). Pure red electrophosphorescence from polymer light-emitting diodes doped with highly emissive bis-cyclometalated iridium(III) complexes, *J. of Organometallic Chemistry* 695: 1972-1978.

Tsuzuki, T. & Tokito, S. (2008). Highly Efficient Phosphorescent Organic Light-Emitting Diodes Using Alkyl-Substituted Iridium Complexes as a Solution-Processible Host Material, *Appl. Phys. Express* 1: 02185-1 – 02185-3.

Tsuzuki, T. & Tokito, S. (2007). Highly Efficient, Low-Voltage Phosphorescent Organic Light-Emitting Diodes Using an Iridium Complex as the Host Material, *Adv. Mater.* 19: 276-280.

Tsuzuki, T., Shirasawa, N., Suzuki, T. & Tokito, S. (2003). Color tunable organic light-emitting diodes using pentafluorophenyl-substituted iridium complexes, *Adv. Mater.* 15: 1455-1458.

Turro, N. J. (1991a). *Modern Molecular Photochemistry*, University Science Books, USA, pp 305.

Turro, N.J. (1991b). *Modern Molecular Photochemistry*, University Science Books, USA, pp 186.

VanSlyke, S. A. & Tang, C.W. (1985). Organic electroluminescent devices having improved power conversion efficiencies, US Patent 4539507.

VanSlyke, S. A., Chen, C.H. & Tang, C.W. (1996). Organic electroluminescent devices with improved stability, *Appl. Phys. Lett.* 69: 2160-2162.

Vanslyke, S. A., Tang, C. W., O'brien, M. E. & Chen, C. H. (1991). Electroluminescent device with organic electroluminescent medium, US Patent 5061569.

Wakimoto, T., Fukuda, Y., Nagayama, K., Yokoi, A., Nakada, H. & Tsuchida, M. (1997). Organic EL Cells Using Alkaline Metal Compounds as Electron Injection Materials, *IEEE Trans. Electron Devices* 44: 1245-1248.

Wang, H. F., Wang, L. D., Wu, Z. X., Zhang, D. Q., Qiao, J., Qui, Y. & Wang, X. G. (2006). Efficient single-active-layer organic light-emitting diodes with fluoropolymer buffer layers, *Appl. Phys. Lett.* 88: 131113-1 – 131113-3.

Williams, E. L. , Haavisto, K., Li, J. & Jabbour, G. E. (2007). Excimer-Based White Phosphorescent Organic Light-Emitting Diodes with Nearly 100% Internal Quantum Efficiency, *Adv. Mater*. 19: 197-202.

Zhou, X., Nimoth, J. B., Pfeiffer, M., Maennig, B., Drechsel, J., Werner, A. & Leo, K. (2003). Inverted transparent multi-layered vacuum deposited organic light-emitting diodes with electrically doped carrier transport layers and coumarin doped emissive layer, *Synth. Met.* 138: 193-196.

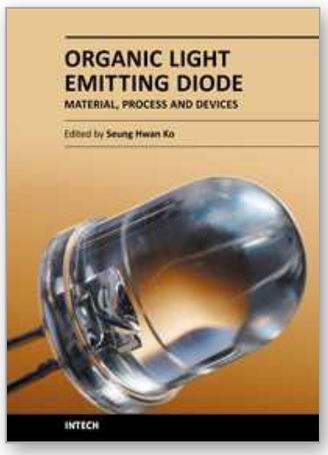

Organic Light Emitting Diode - Material, Process and Devices

Edited by Prof. Seung Hwan Ko

ISBN 978-953-307-273-9
Hard cover, 322 pages
Publisher InTech
Published online 27, July, 2011
Published in print edition July, 2011

This book contains a collection of latest research developments on Organic light emitting diodes (OLED). It is a promising new research area that has received a lot of attention in recent years. Here you will find interesting reports on cutting-edge science and technology related to materials, fabrication processes, and real device applications of OLEDs. I hope that the book will lead to systematization of OLED study, creation of new research field and further promotion of OLED technology for the bright future of our society.

InTech Europe
University Campus STeP Ri
Slavka Krautzeka 83/A
51000 Rijeka, Croatia
Phone: +385 (51) 770 447
Fax: +385 (51) 686 166
www.intechopen.com

InTech China
Unit 405, Office Block, Hotel Equatorial Shanghai
No.65, Yan An Road (West), Shanghai, 200040, China
中国上海市延安西路65号上海国际贵都大饭店办公楼405单元
Phone: +86-21-62489820
Fax: +86-21-62489821

IntechOpen